Dynamical response of the southwestern Laurentide Ice Sheet to rapid Bølling-Allerød warming

Sophie L. Norris[1,2*], Martin Margold[3], David J. A. Evans[4], Nigel Atkinson[5] and Duane G. Froese[2*]

[1]Department of Geography, University of Victoria, David Turpin Building, 3800 Finnerty Road, Victoria, BC, V9P 5C2, Canada
[2]Department of Earth and Atmospheric Sciences, 1-26 Earth Sciences Building, University of Alberta, Edmonton, AB, T6G 2E3, Canada
[3]Department of Physical Geography and Geoecology, Charles University, Albertov 6, 128 43 Praha 2, Czech Republic
[4]Department of Geography, Durham University, South Road, Durham, DH1 3LE, United Kingdom
[5]Alberta Geological Survey, Alberta Energy Regulator, 402 Twin Atria Building, 4 4999-98 Avenue, Edmonton, AB, T6B 2X3, Canada
*Corresponding authors

Correspondence to: Sophie L. Norris (sophienorris@uvic.ca) and Duane G. Froese (duane.froese@ualberta.ca)

Abstract

The shift in climate that occurred between the Last Glacial Maximum (LGM) and the early Holocene (ca. 18-12 ka BP) displayed rates of temperature increase similar to present-day warming trends. The most rapid recorded changes in temperature occurred during the abrupt climate oscillations known as the Bølling-Allerød interstadial (14.7-12.9 ka BP) and the Younger Dryas stadial (12.9-11.7 ka BP). Reconstructing ice sheet dynamics during these climate oscillations provides the opportunity to assess long-term ice sheet evolution in reaction to a rapidly changing climate. Here, we use glacial geomorphological inverse methods (flowsets) to reconstruct the ice flow dynamics and the marginal retreat pattern of the southwestern sector of the Laurentide Ice Sheet (SWLIS). We combine our reconstruction with a recently compiled regional deglaciation chronology to depict ice flow dynamics that encompass the time period from pre-LGM to the early Holocene. Our reconstruction portrays three macroscale reorganizations in the orientation and dynamics of ice streaming followed by regional deglaciation associated with rapid warming during the Bølling-Allerød interstadial. Initial westward flow is documented, likely associated with an early set of ice streams that formed during the advance to the LGM. During the LGM ice streaming displays a dominant north to south orientation. Associated with ice sheet thinning at ~15 ka, a macroscale reorganization in ice stream flow occurred, with a complex of ice streams recording south-eastward flow. A second macroscale reorganization in ice flow is then observed at ~14 ka, in which southwestern ice flow is restricted to the Hay, Peace, Athabasca, and Churchill river lowlands. Rates of ice sheet retreat then slowed considerably during the Younger Dryas stadial; at this time, the ice margin was situated north of the Canadian Shield boundary and ice flow continued to be sourced from the northeast. Resulting from these changes in ice sheet dynamics, we recognize a three-part pattern of deglacial landform zonation within the SWLIS characterized by active ice margin recession and ice sheet stagnation and downwasting punctuated by local surging (terrestrial ice sheet collapse): the outer deglacial zone contains large recessional moraines aligned with the direction of active ice margin retreat; the intermediate deglacial zone contains large regions of hummocky and stagnation terrain, in some areas crosscut by the signature of local surges, reflecting punctuated stagnation and downwasting and; the inner deglacial zone contains inset recessional moraines demarcating progressive regional ice margin retreat. We attribute these macroscale changes in ice flow geometry and the associated deglacial behaviour to external climatic controls during the Bølling-Allerød and Younger Dryas but also recognize the role of internal (glaciological, lithological and topographic) controls.

1 Introduction

Mass loss from contemporary ice sheets and its contribution to rising global sea level has enhanced over the last three decades and is projected to continue to rise (Pattyn et al., 2018). These changes have mainly resulted from accelerated ice-flow rates and changes in surface mass balance, broadly linked to atmospheric and oceanic warming (Alley et al., 2005; Rignot and Kanagaratnam, 2006; Rignot et al., 2008, 2011; Shepherd, 2018). Changes in ice sheet dynamics are of particular concern given the potential sea level equivalent contribution of ice sheets in Greenland and Antarctica (Pattyn et al., 2018). However, with only a few decades of observations, significant uncertainties remain in projecting an ice sheet's response to future climate system changes. Consequently, reconstructing the behaviour of palaeo-ice sheets and how it relates to past climatic change is important to predict future changes to contemporary ice sheets (Alley and Bindschadler, 2001; Rignot and Thomas, 2002; Clark et al., 2009; Carlson and Clark, 2012).

In this context, the complex and largely well-preserved landform imprint of the Late Wisconsinan Laurentide Ice Sheet (LIS) documents regional palaeoglaciological responses to rapid climate change following on from the Last Glacial Maximum (LGM) and consequently is known as an important source of information (Dyke and Prest, 1987; Clark, 1994; Dyke, 2004; Margold et al., 2015b; Stokes et al., 2016; Margold et al., 2018). In particular, geomorphic, sedimentary and geochemical investigations of parts of the southwestern LIS (SWLIS) have documented significant changes in ice flow orientation (Ross et al., 2009; Ó Cofaigh et al., 2010; Evans et al., 2014; Atkinson et al., 2016; Margold et al., 2015b, 2018; Fig 1). However, until recently, large differences between chronological methods have led to uncertainties surrounding the timing of these reorganizations. An updated deglacial chronology (Norris et al., 2022), comprising a synthesis of ~150 ^{10}Be terrestrial cosmogenic nuclide exposure, radiocarbon and infrared/optically stimulated luminescence dates, indicates that the SWLIS underwent rapid deglaciation in response to warming during the Bølling-Allerød (BA) interstadial (14.7-12.9 ka BP; Rasmussen et al., 2014) followed by a decrease in ice sheet retreat rates and marginal stand-still during the Younger Dryas (YD) stadial. Here, we use glacial geomorphological mapping followed by the classification of individual features into flowsets to reconstruct the ice flow dynamics and the marginal retreat pattern of the SWLIS. We combine this ice dynamic reconstruction with existing chronologies to present a model of ice sheet behaviour from pre-LGM to the start of the Holocene.

Our reconstruction supports previous ideas of rapidly switching ice flow directions within the SWLIS during the last deglaciation. We propose that these ice flow changes result from three macroscale ice flow reorganizations within a ~2500 yr interval accompanied by rapid ice margin retreat and ice margin stagnation (in some areas punctuated by local surging). We attribute these macroscale changes in ice flow dynamics, in large part, to climatic changes during the BA and YD. However, we also highlight the complex interplay between this external driving mechanism and internal glaciological, lithological, and topographic controls.

2 Background

2.1 Study area

The SWLIS covered an area of approximately 900,000 km^2 and was located on both the Canadian Shield and the Interior Plains. In the northeast of the region, the Canadian Shield exposes Crystalline lithologies, which in some locations are locally mantled by a surface cover of Quaternary sediment. In the southwest of the region, the Western Canadian Sedimentary Basin overlays the

Canadian Shield, and this thick package of sedimentary rock broadly slopes and thins towards the northeast (Mossop and Shetsen, 2012; Banks and Harris, 2018). In part resulting from the northeasterly thinning of the Western Canadian Sedimentary Basin, the Interior Plains exhibits a pronounced surface gradient that descends from its highest point of 1200 m a.sl. in the west to a low point of 240 m a.s.l at the transition to the Canadian Shield. A network of predominately northwest to southeasterly orientated buried preglacial valleys dissect the landscape and are eroded into the Western Canadian Sedimentary Basin (Stalker, 1961; Cummings et al., 2012). In many locations, preglacial valleys hold thick sequences made up of multiple glacial diamicts and packages of fluvial gravels and glaciofluvial silts, sands and clays (Klassen, 1989; Stalker, 1961; Evans and Campbell, 1995; Andriashek and Atkinson, 2007). Multiple uplands separate this preglacial valley system and rise up to 700 m above the gently sloping surface of the Interior Plains (Leckie, 2006).

2.2 Previous works

The geomorphology and sedimentology of the region encompassed by the SWLIS have been well-studied (Prest, 1968; Christiansen, 1979; Shetsen, 1984; Dyke and Prest, 1987; Evans, 2000; Dyke, 2004; Evans et al., 2008; Fisher et al., 2009; Ross et al., 2009; Ó Cofaigh et al., 2010; Kleman et al., 2010; Evans et al., 2012, 2014; Margold et al., 2015b; Atkinson et al., 2016; Utting et al., 2016; Margold et al., 2018; Evans et al., 2020, 2021). Within the region, cross-cutting landforms, as well as variation in striations, till lithologies and geochemical signatures document changes in ice flow orientation. Relatively older and overprinted southwesterly ice flows have previously been suggested to be associated with an advancing ice sheet (Ó Cofaigh et al., 2010; Margold et al., 2015b). A dominant southern flow has been attributed to LGM conditions, and a subsequent southeastward and then southwest flow was thought to have operated during ice retreat (Evans, 2000; Evans et al., 2008; Ross et al., 2009; Ó Cofaigh et al., 2010; Evans et al., 2012, 2014; Margold et al., 2015b, a, 2018; Evans et al., 2020, 2021). While the reconfiguration of these ice streams can be clearly seen in the geomorphic record, they have not been reconstructed in detail for the entire ice sheet sector. Further, the timing of changes in ice sheet dynamics and how they may relate to external climate forcing or internal forcing mechanisms (i.e., glaciological, lithological, and topographic changes) remains largely undetermined.

Until recently, the deglacial chronology of the SWLIS was based primarily on radiocarbon data (in compilations by; Dyke, 2004; Dalton et al., 2020), the application of which is limited by the unknown temporal offset between deglaciation and biotic colonization (c.f. Froese et al., 2019). Furthermore, where infrared/optically stimulated luminescence dating and a small number of ^{10}Be terrestrial cosmogenic nuclide exposure ages have been used to complement radiocarbon chronologies, significant differences between dating methods have meant that our understanding of the deglacial response of the SWLIS to climate drivers has remained limited. Norris et al. (2022) recently addressed these issues by combining existing luminescence and the most viable minimum-limiting radiocarbon dates with new ^{10}Be exposure ages to establish the timing of SWLIS deglaciation. Within a Bayesian framework, this compilation unified the ages provided by these methods into an internally consistent chronology, which indicates that the SWLIS retreated from its southernmost coalescence with the CIS to its YD position along the Cree Lake Moraine (Fig. 1) in ≤ 2500 yrs (Norris et al., 2022).

Deleted: Bordering the eastern foothills of the Rocky Mountains, the SWLIS subsumed several uplands, which are composed of bedrock remnants of Cretaceous shales and sandstones . Large preglacial valley systems separate these uplands and are composed of thick (up to ~350 m) Quaternary sequences of diamict, glaciofluvial sand and gravel and glaciolacustrine silts and clays

Deleted: geomorphic

Deleted: sedimentological imprints

Deleted: ice flow within

Deleted: documented, with sediment-landform associations, lithological provenance and till geochemistry being used to reconstruct ice stream catchments and flow orientation

Deleted: changes

Deleted: ice stream configuration are prominent in the landform

Deleted: Across the SWLIS, moraines and other ice-marginal landforms relating to ice sheet recession have been the focus of numerous studies .

Deleted: within the Interior Plains are associated mainly with Quaternary vertebrates and

Deleted: unquantified biases

Deleted: ice retreat

Deleted: of the region by plants and animals

Deleted: discrepancies

Deleted: across the region

Deleted: is poorly constrained

Deleted: discrepancies

Deleted: pre-

3 Methods

3.1 Geomorphological mapping

In order to provide a complete reconstruction of the ice flow configuration and dynamics as well as the ice-marginal retreat, the glacial geomorphology of the SWLIS was collated from pre-existing mapping (Ó Cofaigh et al., 2010; Atkinson et al., 2014; Evans et al., 2016; Norris et al., 2017; Atkinson et al., 2018; Evans et al., 2020). The following landform categories were collated from pre-existing mapping: ice flow parallel lineations (drumlinoid ridges, mega-scale glacial lineations (MSGL), and crag-and-tail features), moraine crests (lateral shear, terminal and recessional), ice-thrust ridges (and glaciotectonic rafts), crevasse fill ridges, meltwater channels and eskers, kames/hummocks, palaeo-shorelines, dunes and undifferentiated ridges. Pre-existing mapping comprises features that were predominantly identified from satellite imagery combined with detailed aerial photograph interpretation. In many locations, features have been ground-truthed by the original authors (e.g. Matthews et al. 1975; Atkinson et al 2014, 2018 and references therein). In particular, geomorphic mapping from LiDAR imagery (5-15 m resolution) at a 1:10,000 scale was utilized for Alberta (Atkinson et al., 2014, 2018). For all other parts of the study area, geomorphic mapping was compiled at 1:30,000 (Norris et al., 2017), 1:10,000 (Ó Cofaigh et al., 2010; Evans et al., 2016, 2020) and 1:1,000,000 (Mathews et al., 1975) scales. Resulting from an absence of LiDAR data within Saskatchewan and northeast British Columbia, mapping has been primarily completed from a combination of 1-arc second SRTM (~30 m resolution), ALOS (~30 m resolution) imagery and aerial photograph analysis.

3.2 Glacial inversion (flowset classification)

We utilized a glacial geomorphological inversion method or flowset approach (see Kleman and Borgström, 1996; Kleman et al., 1997, 2006; Greenwood and Clark, 2009), which formalizes standardized geomorphological mapping techniques (Dyke et al. 1992). The approach applies our pre-existing knowledge of landform generation to allow us to reconstruct ice sheet properties using features formed at the bed of a palaeo-ice sheet (Fig. 2) (Kleman et al., 1997, 2006). Ice flow patterns were grouped into flowsets based on their morphometry and proximity to other glacial landforms (Clark, 1999). The degree of orientation similarity in lineation was also taken into account, following the assumption that all lineations in the same flowset should have similar orientations (Clark, 1999). Following the procedures outlined by Atkinson et al. (2016), glacial inversion methods were combined with a landsystems approach (see Evans, 2007, 2013). This enables landforms and their constituent sediment to be combined into assemblages related to genetic processes, which facilitates a more comprehensive evaluation of 'process form' to be included in the assessment of palaeo-ice sheet and ice streaming dynamics (Evans et al., 2008, 2014; Atkinson et al., 2016; Fig. 2). To make determinations about the sediments that comprise landforms, we utilised previously published surficial geology mapping (Simpson, 1997; Fenton et al., 2013; Geological Survey of Canada, 2014; Bednarski, 2000; Hickin and Fournier, 2011).

We synthesized and updated flowsets (mapped and originally presented by Evans et al., 2014; Atkinson et al., 2016; Utting et al., 2016; Norris, 2019; Atkinson and Utting, 2021) and generated new flowset mapping in regions where no mapping was available (~25% of the flowsets) (Fig. 3a). In addition to mapped glacial geomorphology, in many cases, previous regional scale delineation of ice flow corridors or ice stream locations guided our flowset identification (Evans, 2000; Ross et al., 2009; Evans et al., 2008; Ó Cofaigh et al., 2010; Evans et al., 2012; Margold et al., 2015b, a; Stokes et al., 2016; Margold et al., 2018; Evans et al., 2020) (Fig. 3a). Each flowset was then divided into one of six categories: (i) ice stream, (ii) event, (iii) deglacial retreat, (iv) deglacial readvance, (v) palimpsest and (vi) unknown (Table 1, categories adapted from Kleman, 2006). Flowsets were then ordered

according to their relative age based on their cross-cutting relations (Kleman et al., 2006; Greenwood et al., 2007; Greenwood and Clark, 2009; Kleman et al., 2010; Hughes et al., 2014) to reconstruct dynamics changes in ice flow over time.

270 Consistent with previous studies within the Canadian Prairies (e.g. Ross et al., 2009; Ó Cofaigh et al., 2010; Margold et al., 2015b; Stokes et al., 2016), we refer to an 'ice stream' as a corridor within an ice sheet that is flowing relatively faster than the ice surrounding it. We also document switches between periods of rapid ice flow and slower ice flow likely driven by internal forcing mechanisms; in such cases, we refer to them as exhibiting 'surge' behaviour (Evans et al., 1999; Clayton et al., 1985; Evans et al., 2020) and classify them as deglacial readvance flowsets.

275

3.3 Deglacial dynamics

We place our reconstruction into a chronological context using the ice margin chronology of Norris et al. (2022). This dataset comprises ~150 [10]Be terrestrial cosmogenic exposure ages, infrared/optically stimulated luminescence, and high-quality, minimum-limiting radiocarbon ages. These data were combined within a Bayesian statistical framework to present an internally
280 consistent retreat chronology. We combine this chronology with the mapped ice margin positions of Dyke (2004) and Dalton et al. (2020), reassigning a new age to each position based on the chronology of Norris et al. (2022), and present recessional isochrones for the SWLIS.

4 Results

We identify 425 flowsets in the SWLIS landform record (Fig. 3b; to view individual flowsets discussed below, see the supplemental
285 .kml file in Google Earth). We present flowsets and their constituent landforms, which have been identified from previous studies (mapped and originally presented by Evans et al., 2014; Atkinson et al., 2016; Utting et al., 2016; Norris, 2019; Atkinson and Utting, 2021) and delineated flowsets from geomorphological mapping where none existed (Fig. 3a). All flowsets were then categorized as either (i) ice stream, (ii) event, (iii) deglacial retreat, (iv) deglacial readvance, (v) palimpsest and (vi) unknown (Table 1) and differentiated based on relative age.

290

Of the 425 flowsets mapped, we categorized ~55% of flowsets ice stream, 11% as event, 13% as deglacial retreat, 9% as deglacial readvance and 8% as palimpsest flowsets. ~20 flowsets (4%) contained only a small number of landforms that are fragmented or whose origins are unclear, we categorize these flowsets as having an unknown origin. Recorded by the cross-cutting relationships of flowsets, it is clear that ice flow patterns within the SWLIS document several macroscale reorganizations (Fig. 3b). Below, we
295 present the evolution of ice flow in five phases. While we differentiate our reconstruction into five major phases, we note that in many cases, flowsets document a time-transgressive bedform generation (see Greenwood and Clark, 2009) and reflect a rapidly fluctuating ice flow regime. As such, multiple flowsets may depict ice flow in a small region during a single phase. In these cases, the relative timing of flowset evolution is described below and documented in Figure 4.

4.1 Phase 1

300 Phase 1 documents ice flow from the northeast to the southwest. It comprises 25 flowsets (Fig. 4a) composed of drumlins and flutings. These flowsets are not associated with any ice-marginal landforms. Their imprint is mainly preserved in areas of high

ground. They occur as topographically unconstrained southwestward-oriented fast-flow corridors extending for up to 60 km across the Cameron Hills (fs417), Birch Mountains (fs267), Clear Hills (fs300, 348, 349, 353, 355, 358, 362, 369, 379, 388, 390), Stony Mountain (fs123, 130, 157 and 181), Buffalo Head Hills (fs330), and Swan Hills (fs245). Within the eastern portions of the study area, fs10 and 6 record southwestward flow restricted to the valley base, northeast and southwest of Saskatoon and fs 134 and 141 record southwestward flow northeast of Edmonton. Sourced from the Rocky Mountains, northwest-orientated ice flow is recorded within the Grande Prairie region (fs 310, 324, 361).

4.2 Phase 2

Phase 2 documents ice flow from north to south (Fig. 4b) in multiple corridors. Within the western portions of the study area during this phase, fs191, 197, 198, 200, 209, 212, 214, 219, 220, 223, 278 and 281 document a series of tributary flows that coalesce in the Athabasca River lowlands as a single flowpath (fs207). These flowsets comprise a high density of MSGL as well as drumlins and flutings. This single major north-to-south aligned flow separates immediately north of Edmonton. It can be traced over 450 km as an eastern corridor (f38,51,93,142) and western corridor (fs39, 57, 58, 76, 104, 111, 119, 121, 129, 148, 152, 151, 153, 160, 167, 170, 172, 186, 189, 192, 201,204, 208) both of which end in extensive zones ice marginal landforms (Lethbridge moraine complex; Stalker, 1962, 1977; Eyles et al., 1999; Evans et al., 2008, 2012, 2014). Cordilleran ice draining to the southeast from the Rocky Mountains is documented by fs55, 59, 68, 70, 75, 80, 84, 87, 90, 91, 168, 170, 174, 190, 213, 242, 248, 262, 265.

Within Saskatchewan, north-to-south oriented ice flow is first documented as a small flowset (fs 137) composed of drumlins located at the southwest boundary of the Canadian Shield. Flow can then be traced to a region of widespread southwest-trending MSGL (fs42, 54, 61, 62 and 67). This flow path then extends along the Alberta-Saskatchewan border as a succession of seven flowsets (fs12, 16, 18, 19, 24, 30, 42), ending at a series of stacked moraines on the northern side of the Cypress Hills. In several locations, lineations comprising these flowsets are overprinted by concentrations of crevasses fill ridges. South of the Cypress Hills, fs5,7 and 8 document evidence of small ice flows that extend around this upland to the south.

4.3 Phase 3

Phase 3 documents ice flow from the northwest to southeast (Fig. 4c). Large regions of streamlined subglacial bedforms occur over six broad corridors. These corridors separate the widespread hummocky terrain (in some places locally overprinted by surge-type geomorphic signatures) that characterizes much of the central SWLIS. In several locations, these streamlined zones are overprinted by swaths of crevasses fill ridges that are oriented perpendicular to the ice flow direction. In addition, the boundary of these fast-flow corridors is often demarcated by 'ice stream or lateral shear moraines' (see Ross et al., 2009; Ó Cofaigh et al., 2010).

Within the northern portions of the Churchill River lowlands, fs26, 34, 40, 85, 149 and 150 record ice flow that cross-cuts Phase 2 southerly oriented flow. The flow direction of bedforms that comprise these flowsets is difficult to identify because they are overlain by glaciolacustrine material. However, multiple ice thrust ridges that are accompanied by small up-ice hollows (hill-hole pairs) throughout this region indicate ice flow to the southeast. Within the southern portions of the Churchill River lowlands, fs4, 52, 81, 97, 106, 112, 124, 127, 128, 136, 145, 154, 158, 163, 166, 177, 178 record a similar ice flow that originated northwest of

Cold Lake. Areas north and south of the Neutral Hills display similar southeastward-oriented flow as documented by fs28 and 43. This ice flow was subsequently cross-cut by a slightly later south-southeast ice flow (fs 2, 3, 9, 25 and 66).

Closer to the western ice margin at this time, ice flow fed lobes in the Calgary (fs 72, 74, 82, 92, 99, 102, 116, 121, 131, 144, 148, 151, 160, 162, 167, 172, 179, 180, 192, 193, 202 and 208) and Lethbridge regions (fs 11, 13,14,15, 21, 22, 23, 27, 29, 31, 35, 38, 41, 44, 46, 47, 50, 51, 53, 93, 95, 100, 133, 138, 147), recording southwestward ice flow orientations. Within the Grande Prairie region, small ice lobes were fed by Cordilleran (fs 213, 265, 272, 354) and Laurentide ice (fs250, 280, 288, 291, 296, 304, 305, 314, 320, 341, 342, 363). In several areas, overprinting of these wide ice flow corridors occurs. These are best documented surrounding the Neutral Hills, where flowsets appear to have been sourced from the upland and overprint parts of the regional scale southwestward flows within the surrounding lowlands (e.g., fs 32,33 48, 60, 79, 88, 98, 110). In several cases, these flowset overprint or are composed of glaciolacustrine material, suggesting that proglacial lakes were present in the landscape during their formation.

4.4 Phase 4

Phase 4 documents southwestward oriented ice flow in the Hay (e.g., fs384, 396, 398, 419, 425), Peace (e.g., 308, 317,326 and 335) and Athabasca (e.g., fs 211,214,219, 222, 227, 236, 244, 254 and 255) river lowlands (Fig. 4d). The geomorphic imprint of southwesterly ice flow is also visible on the upper surface of the Birch Mountains (fs 253 and 264). Within the Churchill River lowlands, a southeastward flow is recorded (fs 25, 49, 77, 83, 125 and 146) (Fig. 4d). On a local scale, several small-scale shifts in ice flow direction as documented during this phase. Firstly, associated with fs 150, the cross-cutting relationship of two well-preserved lateral shear moraines reveals a progressive 'clockwise' migration of ice flows. This cross-cutting pattern likely signifies a shift in the ice drainage migrating from a west-to-north source as the ice sheet thinned over the Stony Mountains (i.e., from Phase 3 to 4). Secondly, fs146 and 125 document another local ice flow migration. These flowsets document a shift from southwestward ice streaming to northwestward ice flow (feeding flows within the Hay and Peace River ice flows). Glacial lineations in these flowsets blend with one another, implying a migration rather than a simple overprinting (see also Margold et al., 2015a, b, 2018). It should also be noted that a similar time transgressive 'clockwise' migration of ice flow and lateral shear moraines is also observed immediately east of the SWLIS by Ross et al. (2009) in the region south of Prince Alberta, Saskatchewan.

4.5 Phase 5

Phase 5 documents the last stages of ice flow to the southwest (Fig. 4e). During this phase, ice flow terminated at the Cree Lake Moraine and Upper Cree Lake Moraine complex. A large regional scale flowset (fs 164) and a series of smaller retreat and localized readvance flowsets (fs 65, 77, 94, 101, 114, 118, 135, 140 and 161) cover areas of the exposed crystalline bedrock of the Canadian Shield as well as regions covered by patches of Quaternary sediment.

In addition to flowsets associated with regional deglaciation, this phase documents ice draining radially from several uplands. Flowsets on the Cameron Hills (fs 418, 424), Caribou Mountains (fs 332, 339, 352, 356), Birch Mountains (fs 260 and 275), Clear Hills (fs 368, 373, 376) and Swan Hills (fs 274) comprise suites of lineations and ice-marginal channels, eskers and recessional moraines that overprint flowsets documenting regional deglaciation (phase 4 flowsets). These landforms also cross-cut recessional moraines and glaciolacustrine sediments within the surrounding lowlands, suggesting that the lowland regions were ice-free and that proglacial lakes in the area had drained (see also, Atkinson et al., 2016).

5 Dynamic evolution of the SWLIS

To place our ice sheet reconstruction into chronological context, we integrate our flowset and ice-marginal geomorphologic mapping with the deglacial chronological synthesis of Norris et al. (2022). We combine this ice margin chronology with the mapped ice margin positions of Dyke (2004) and Dalton et al. (2020), reassigning a new age to each position based on the chronology of Norris et al. (2022), and reconstruct ice sheet dynamics and configuration at five phases spanning pre-LGM to early Holocene (Fig. 4).

5.1 Pre-LGM ice flow pattern (Phase 1)

Phase 1 flowsets likely document the advance towards convergence of the CIS and LIS before the LGM. In many cases, flowsets relating to this phase are small and fragmented. To avoid overinterpretation of the geomorphic record, we do not delineate ice stream pathways associated with the pre-LGM ice flow pattern, however in regions where these have previously been identified, we include them in our interpretation (see Fig. 4). Evidence for southwestward fast flow relating to this phase is largely restricted to upland areas (Buffalo Head, Cameron, Clear and Swan Hills and Birch and Stony Mountains) within the central portion of the SWLIS (Fig. 4a). Flowsets on the Cameron Hills are broadly consistent with a region of ice streaming highlighted by Margold et al. (2015a, b) and are interpreted as their 'Cameron Hills Fragments'. Within the eastern part of the study area, southwestward flow is also preserved in the lowland regions surrounding Saskatoon and northeast of Edmonton. Portions of our flowsets in these regions have previously been noted by Ó Cofaigh et al. (2010) and Margold et al. (2015a, b) and we interpret our flowsets as an extension of their 'Pre 1 Fragments' and 'Winefred Lake Fragments', respectively. Initial convergence between the LIS and CIS is recorded in the Grande Prairie region. These flows were originally delineated into flowsets by Atkinson et al. (2016) and depict that initial eastward flows have been deflected northwestward, likely by the LIS. Subglacial landforms that comprise flowsets in the Grande Prairie and Calgary regions have been interpreted by Atkinson et al. (2016) to signify synchronous build-up of the CIS and LIS. We support this interpretation and suggest that these flowsets must have been active prior to the formation of an extensive CIS-LIS ice saddle, which would have deflected ice flow to the south.

Within southern Alberta, we do not document any flowsets relating to this phase, although 'overridden glaciotectonic composite ridges' have been mapped previously in the region (see Evans et al., 2008, 2012, 2014). These landforms demarcate the lobate margins of what would become major LGM ice stream tracks (see Evans et al., 2008, 2012, 2014). Minimal chronology relating to the pre-LGM ice sheet evolution of the SWLIS is available. However, a southwestward ice flow orientation is consistent with previous continental-scale reconstructions (Dyke et al., 2002; Batchelor et al., 2019; Dalton et al., 2022) of pre-LGM buildup following Marine Isotope Stage 3. This interpretation also agrees with till geochemical analyses that show calcium oxide concentrations to be elevated in tills across southeastern Alberta, which have been linked to a dolomite boulder dispersal train extending over >100 km from central Saskatchewan (Westgate, 1968; Pawluk and Bayrock, 1969).

5.2 LGM ice flow pattern (Phase 2)

During the LGM, flowsets record the development of three north to south-oriented ice streams. This ice flow orientation is broadly consistent with previous regional geomorphic reconstructions (Ross et al., 2009; Ó Cofaigh et al., 2010; Margold et al., 2015b, a, 2018; Evans et al., 2008, 2014) (Fig. 4b) and supports the notion of an extensive ice dome and ice (divide) saddle situated to the north (Dyke and Prest, 1987; Margold et al., 2015b, 2018; Tarasov et al., 2012). Within the eastern portion of the SWLIS, we document the flowpath of the region's most longitudinally extensive ice stream. This ice stream flowpath was first mapped by

Prest et al. (1968) and formally identified as the East Lobe by Shetsen (1984) and later delineated by Ross et al. (2009) as the Maskwa Corridor and by Ó Cofaigh et al. (2010) as Ice Stream 1. To avoid confusion, we herein refer to this flowpath as the Maskwa Ice Stream (Maskwa IS). The onset zone of the Maskwa IS is cross-cut by later ice flows and is only preserved as a single flowset (fs137). We suggest this flowset documents the southern portion of the convergent flow that sat north of the Canadian
545 Shield boundary. An onset zone near the Canadian Shield boundary is also supported by regional airborne gamma-ray spectrometry surveys (GSC, 2008; Ross et al., 2009), which document the distribution of potassium-rich glacial diamict transported from the Canadian Shield along a north-to-south flowpath that is broadly aligned with fs137.

The Maskwa IS extended from its onset zone and ended on the northern side of the Cypress Hills (after Ross et al., 2009; Ó Cofaigh
550 et al., 2010; Margold et al., 2015b, 2018). The geomorphic imprint of the Maskwa IS on the Cypress Hills likely correlates to the highest elevation of the Elkwater drift recorded on this upland (see Westgate, 1968; Evans et al., 2014). Transporting ice flow south, the Maskwa IS fed two small ice lobes that flowed around the east and west of the Cypress Hills (herein named East and West Cypress Hills fragments) (Klassen, 1994; Ross et al., 2009; Ó Cofaigh et al., 2010; Evans et al., 2016).

555 Within the Athabasca River lowlands, we document the onset zone of another north-to-south oriented ice stream. Due to its association with previous work further to the south (Prest et al., 1968; Evans et al., 2008; Atkinson et al., 2014), we interpret this as the onset zone of the Central Alberta Ice Stream and High Plains Ice Stream (hereafter CAIS and HPIS) (Prest et al., 1968; Evans, 2000; Evans et al., 2008; Margold et al., 2015a, b). These ice streams flowed as a single pathway until they separated immediately northeast of Edmonton, the western arm becoming the HPIS. The HPIS then merged with ice flowing from the CIS
560 to form the Rocky Mountain Foothills Ice Stream (Evans et al., 2008, 2012, 2014; Utting et al., 2016; Margold et al., 2015b, 2019). The onset zone of the CAIS/HPIS in the Athabasca River lowlands region does not display a zone of convergent flow (i.e. Prest et al., 1968; De Angelis and Kleman, 2008). While it is possible that the zone of convergence for these ice streams may not have been preserved in the geomorphic record (e.g., Evans et al., 2014) we instead suggest that it did not have a convergent onset zone while active, but rather was sourced by multiple smaller feeder tributaries. This is justified by the small changes in ice stream
565 orientation recorded within the Athabasca River lowlands and the existence of multiple flowsets (e.g., fs198, 214, 261, 278 and 281), which feed into this region.

In line with previous reconstructions, we suggest that the SWLIS would have drained via the Maskwa IS, CAIS, HPIS, and Rocky Mountains Foothills IS following the development of the Keewatin Ice Dome and CIS-LIS saddle and thus likely the maximum
570 buildup of the coalescence zone between the CIS-LIS (Dyke and Prest, 1987; Margold et al., 2015b, 2018). While the age of ice stream initiation is not well known, below till radiocarbon dates in central Alberta indicate that they must postdate the incursion of the SWLIS into the region after ~25 ka BP (Young et al., 1994).

In contrast to other sectors of the LIS, LGM ice streaming in the SWLIS flowed unconstrained by topography (Ross et al., 2009;
575 Ó Cofaigh et al., 2010; Margold et al., 2015b, 2018). This has been suggested by previous studies to result from the large ice thicknesses over the SWLIS due to its proximity to the southwestern portion of the Keewatin Ice Dome, (Ross et al., 2009; Ó Cofaigh et al., 2010; Margold et al., 2015b, 2018). Additionally, unlike other sectors of the LIS, the lack of large troughs or valleys throughout the region would have meant the SWLIS was predisposed to having ice streams unconstrained by topography in the presence of extensive ice thickness (Ross et al., 2009; Ó Cofaigh et al., 2010; Margold et al., 2015b, 2018). Numerical models
580 estimate average LGM ice thicknesses in these regions vary from >1500 to <2000 m (Tarasov et al., 2012; Peltier et al., 2015;

Gowan et al., 2016; Lambeck et al., 2017). Similar ice thicknesses are also evidenced by observations of glacial isostatic adjustment observed through mapping of postglacially delevelled lake shorelines (e.g. glacial lakes Agassiz and McConnell) (Breckenridge, 2015).

5.3 Rapid downwasting of the LIS and CIS convergence zone (Phase 3)

We map 103 flowsets associated with this ice flow phase that documents a shift from north to south-oriented LGM flows to southeasterly flows (Fig. 4c). Many of these flows have been mapped and interpreted previously as the product of a macroscale switch in the ice dynamics associated with rapid ice sheet thinning and downwasting of the CIS-LIS convergence zone (Ross et al., 2009; Ó Cofaigh et al., 2010; Margold et al., 2018). Southeastward ice flows within the SWLIS were first highlighted by Ross et al. (2009) and Ó Cofaigh et al. (2010), who documented IS2 (Buffalo Corridor of Ross et al., 2009) that cross-cut the Maskwa IS. We document these ice streams and map similar southeastward-oriented flows northeast of the Mostoos Hills and north of the Cypress Hills (we herein refer to this collection of ice streams as the IS2 complex) (Fig. 4c).

The change from the topographically unconstrained system of the Maskwa IS, CAIS and HPIS to the topographically constrained southeastward flow of the IS2 complex has been proposed to reflect CIS-LIS saddle collapse and rapid ice downwasting centred in the CIS-LIS convergence zone (Fig. 4c) (Margold et al., 2018). Thinning of the CIS-LIS convergence zone is constrained by [10]Be terrestrial cosmogenic exposure dating from the northwest LIS, indicating that the region underwent rapid surface thinning starting at ~14.9-14.3 ka BP (Stoker et al., 2022). In addition, numerical model simulations (Tarasov et al., 2012; Gregoire et al., 2016) suggest that thinning and initial separation of the CIS and LIS occurred extremely rapidly, broadly correlated with the start of BA warming (ca. 15 ka BP) (Gregoire et al., 2016; Stoker et al., 2022). We note, however, that during this ice flow phase, an ice divide extending from the Keewatin Ice Dome to the west must have remained (at least in part) present to support flow in a southeastward direction (see also Ross et al., 2009; Margold et al., 2015b, 2018). Due to substantial ice thinning, this ice divide would no longer have been fed by ice draining across the Rocky Mountains (Margold et al., 2018), so we no longer refer to it as the CIS-LIS saddle. Instead, this divide would have been situated broadly over the Caribou Mountains in northern Alberta (precise position undefined) and is herein referred to as the Plains Ice Divide (after Dyke and Prest, 1987).

Following the initial separation of the LIS and CIS, the SWLIS experienced rapid downwasting and retreat (Norris et al., 2022). Comparing the initial position of multiple south-eastward flowing networks, we agree with the previous suggestions of Ross et al. (2009), Ó Cofaigh et al. (2010) and Margold et al. (2015b, 2018) who proposed that these ice streams would have stopped after the development of a deglacial corridor, commonly referred to as the 'ice-free corridor', between the CIS-LIS; otherwise, the ice streams would have lacked an accumulation zone to drive flow southeastward. Norris et al. (2022) suggest the timing of LIS retreat across the Interior Plains also implies that following initial detachment from the CIS, rapid retreat rates (380-340 m/yr) continued to characterize SWLIS deglaciation, contemporaneous with BA warming. This chronology suggests that southeasterly-oriented ice flows (IS2 complex) would have been very short-lived, operating for as little as ~500 yrs before they stopped and westerly flows became active in their place as the ice margin retreated.

5.4 Deglaciation of the Interior Plains (Phases 4 and 5)

5.4.1 CIS-LIS separation

Our flowset mapping, in combination with previous detailed geomorphic mapping by Evans et al. (2014) suggests that concurrent with initial separation, the lobate margins of the HPIS, CAIS and Maskwa IS experienced a predominantly active recession, as

documented by the Frank Lake, Lethbridge and Cypress Hills moraine complexes, respectively (Fig. 4d). Zones of linear hummocky moraine (controlled moraine) and push moraine ridges that comprise these ice-marginal complexes suggest that the ice-stream margin underwent repeated switches between polythermal and warm-based conditions during ice retreat (Evans et al., 2014). North of the Lethbridge moraine, flowsets that mark the recession of the HPIS are, in some places, partially overprinted by ice thrust ridges ('thrust moraines' of Evans et al. 2014) a secondary set of lineations sourced from the CAIS; this landform assemblage supports the previous detailed geomorphic mapping and sedimentological observations of Evans et al. (2008, 2014) of a later-stage CAIS fast flow event in this region (Fig. 4d). During the separation of these two ice lobes regional drainage would have been blocked, which would have resulted in multiple small ice-dammed glacial lakes forming at the margin of the HPIS (e.g. glacial lake Cardston, see Bretz, 1943; Horberg, 1952; Utting and Atkinson, 2019) and the CAIS (e.g. glacial lake Beiseker and Bassano; see Utting and Atkinson, 2019).

The timing of the initial separation of the CIS and the LIS is constrained based on a synthesis of ^{10}Be terrestrial cosmogenic nuclide exposure, radiocarbon and infrared/optically stimulated luminescence dates that span Alberta-British Columbia border zone (Norris et al., 2022). This chronology suggests that the SWLIS's initial separation began at ~14.9 ka BP (Margold et al., 2019; Norris et al., 2022). Interestingly, ^{10}Be exposure ages from additional sites in northwestern Alberta and northeastern British Columbia suggest slightly later separation of the two ice sheets at ~13.8 ka BP (Clark et al., 2022b). We do not adjust our timing of initial CIS-LIS separation based on these additional sites but rather continue to use an age of ~14.9 ka BP because this age is supported by three different geochronological techniques displaying internally consistent results (Norris et al., 2022). However, we emphasise that the inclusion of these additional ^{10}Be exposure sites from Clark et al. (2022b) would imply that the deglaciation of the SWLIS occurred even more rapidly than previously thought, and thus, the ice dynamical switches discussed below would span an even shorter timescale.

5.4.2 Deglaciation of central Alberta and Saskatchewan

The geomorphic record in the central portions of Alberta and Saskatchewan (i.e. northeast of Calgary) suggests deglaciation of the region was the result of widespread stagnation in places punctuated by localized surging (Fig. 5). Within the ice stream trunk zones of the CAIS, Maskwa IS, and IS2 and 3, ice sheet stagnation is demarcated by regions of lineations (MSGL, drumlins and flutes) which are overprinted by crevasse fill ridges (Ó Cofaigh et al., 2010; Evans et al., 2016). Preservation of crevasse fill ridges during active ice recession is very uncommon; therefore, their presence in central Alberta and Saskatchewan indicates that ice in this region likely downwasted in place rather than undergoing step-back recession (Sharp, 1985; Evans, 2007; Evans et al., 2016). Bordering the flowpaths of the ice streams described above, large zones of hummocky terrain cover the landscape. Consistent with the work by Ross et al. (2009) and Ó Cofaigh et al. (2010) we suggest that ice stagnation here resulted from ice stream switching and the scavenging of the central portions of the CAIS and Maskwa IS from their accumulation zones by evolving these southeastward ice flows (IS2 complex). The short-lived southeastward flows of the IS2 complex would also have ceased following CIS-LIS separation (Ross et al., 2009; Margold et al., 2018). Thus, the ice margin in this region would no longer have been nourished, and ice stagnation would have been widespread.

In some locations, flowsets comprised of ice thrust ridges, moraines, lineations and hummocky terrain locally cross-cut large the palaeo-ice stream footprints (Bretz, 1943; Evans, 2000; Evans et al., 2008, 2014, 2016, 2020; Ó Cofaigh et al., 2010). This is particularly evident in central Alberta, at the termini of fs 100, 138, 147 (northeast of Red Deer) and the region surrounding the Neutral Hills demarcated by fs 33,48 and 60 (Evans et al., 2008; Atkinson et al., 2018; Utting and Atkinson, 2019; Evans et al.,

2020). These landforms confirm the development of small surging ice lobes often sourced from upland regions during ice sheet stagnation. In agreement with previous work, we suggest this behaviour was most likely conditioned by the increased availability of subglacial meltwater and/ or the expansion of local proglacial lakes around areas that contained downwasting ice (Evans et al., 2008, 2020; Utting and Atkinson, 2019). Radiocarbon dates suggest the development of biologically viable conditions over the central SWLIS by ~13.3 ka BP (e.g. Edmonton region; Heintzman et al., 2016; Norris et al., 2022). [10]Be exposure, luminescence, and radiocarbon dates indicate that there were ice-free conditions as far north as the city of Cold Lake by ~13.5 ka BP (Norris et al., 2022). We, therefore, suggest that deglaciation, predominantly via large-scale ice sheet stagnation and downwasting in central Alberta and Saskatchewan occurred rapidly at 13.5 ka. However, we note that portions of the landscape may have remained 'ice-cored' for much longer (see section 6.3.2).

5.4.3 Deglaciation of northern Alberta and Saskatchewan

Within the Churchill, Athabasca, Hay and northern portions of the Peace river lowlands, we observe widespread active retreat of the ice margin, fed by southwestward ice streaming of the Hay, Peace and Athabasca ice streams (after Margold et al., 2015b) and southeastward ice streaming of Ice Stream 4/5 (IS4/5) (after Ó Cofaigh et al., 2010) (Fig 4d. We also document small time-transgressive changes in the direction of these ice streams (e.g., northeast of the Caribou Mountains feeding the Buffalo Ice Stream of Margold et al. (2015b, 2018) and on the Stony Mountains feeding IS4/5). As noted by Margold et al. (2015b), these ice streams were initially unconstrained by regional topography, as evidenced by ice stream flow over the Birch Mountains. However, our flowset mapping and the previous large-scale reconstructions of Margold et al. (2018) suggests these ice streams were gradually restricted to the southwestward-oriented valley systems due to ice sheet retreat and thinning. This transition is marked by a series of overprinted flowsets in the Athabasca River lowlands that document the time-transgressive alteration and increasing influence of topographic controls as the ice sheet thinned.

Within all four lowlands, arcuate moraines record ice-marginal recession as a series of small lobes (Fig. 4e; Christiansen, 1979; Fisher et al., 2009). Ice retreat in these lowlands led to the development of several large glacial lakes (Fig. 6). Within the Peace River lowlands the Peace and Wabasca lakes occupied the region immediately in front of the ice margin on the north and south sides of the Buffalo Head Hills, respectively (Utting and Atkinson, 2019). In the Athabasca River lowlands glacial Lake Algar was the first lake to occupy the region (Utting and Atkinson, 2019). Following progressive ice retreat in the Athabasca and Churchill river lowlands, Glacial Lake McMurray/Meadow occupied the region and the Beaver River Moraine demarcates the position of the ice margin at this time. (Fig. 6; Christiansen, 1979; Fisher et al., 2009; Anderson, 2012; Utting and Atkinson, 2019). Glacial Lake McMurray/Meadow would have continued to expand until the ice margin was far enough to the northeast to facilitate drainage either into Glacial Lake Agassiz to the southeast (see below) or Glacial Lake McConnell to the north (Fig. 6; Lemmen et al., 1994; Fisher et al., 2009; Utting and Atkinson, 2019).

[10]Be terrestrial cosmogenic exposure dating suggests that the northern portion of the Athabasca River lowlands (the region surrounding the Clearwater Lower Athabasca Spillway, see Fig. 4d for location) was ice-free by ~13.0 ka BP (Norris et al., 2022). This supports luminescence chronologies from the same region that encapsulate a broader but consistent timing of deglaciation (Munyikwa et al., 2017, 2011; Woywitka, 2019). In contrast, radiocarbon dates within the Athabasca River lowlands indicate deglaciation occurred almost 3 ka later, at ~10.7-10.3 ka BP (Dyke, 2004; Fisher et al., 2009; Dalton et al., 2020; Norris et al., 2022). However, compared to older, more southerly luminescence and radiocarbon dates, these samples provide only minimum-limiting ages for biological productivity in the region (Froese et al., 2019; Norris et al., 2022). In contrast to the Athabasca River

825 lowlands, there are limited chronological constraints within the northern portions of the Peace and Churchill river lowlands. However, based on the geometry of ice-marginal landforms, ice streaming would have been largely synchronous in all three of these lowlands.

5.4.4 Younger Dryas ice flow pattern and deglaciation

830 The YD position of the SWLIS is demarcated by the Cree Lake Moraine and Upper Cree Lake Moraine, located immediately up ice of the Canadian Shield boundary (Fig. 4e). [10]Be terrestrial cosmogenic exposure dating from two sites located on the crest of the Cree Lake Moraine and Upper Cree Lake Moraine (herein Cree Lake Moraine complex) indicate the region was ice-free at ~12.7 ka BP and 12.3 ka BP, respectively (Norris et al., 2022). Concurrent with ice retreat to the Cree Lake Moraine complex position, Glacial Lake Agassiz occupied the Churchill River lowlands to a maximum elevation recorded by shorelines (Fisher and

835 Smith, 1994; Murton et al., 2010; Breckenridge, 2015; Young et al., 2021). Ice sheet stabilization at the Cree Lake Moraine complex would have permitted drainage of Glacial Lake Agassiz through the Clearwater Lower Athabasca Spillway (Fig. 6) to the northwest at some point during the YD stadial (Norris et al., 2021). [10]Be terrestrial cosmogenic exposure dating <50 km northeast of the Cree Lake Moraine complex document deglaciation by 11.2 ka BP, suggesting a stillstand of ~1 ka during the YD. Unlike the lobate, topographically constrained ice flows that occurred in the Churchill, Athabasca and Peace river lowlands as the ice

840 margin retreated onto the Canadian Shield, it was fed by a regionally extensive fast ice flow event that spread across the region as a broad sheet flow (Fig. 4d) (Margold et al., 2015b, 2018).

In addition to ice flow on the Canadian Shield, we recognize evidence of ice caps that persisted after regional deglaciation on the Birch and Caribou Mountains and Cameron and Clear Hills (Fig. 4e). Similar evidence is also documented on the Swan Hills,

845 previously identified by Atkinson (2009) and Atkinson et al. (2016) who document ice flow on the upland after glacial lake drainage. In these five locations, moraines and meltwater channels that document flow into the surrounding lowlands cross-cut older flowsets as well as glaciolacustrine material. Based on the overprinting relationships of landforms on these uplands, we suggest that these ice caps dispersed lobes across the surrounding lowlands after regional-scale ice retreat and the drainage of proglacial lakes (Fig. 6). Although no chronology is available to constrain the timing of their operation, based upon their location

850 relative to regional deglacial isochrones, ice from a dispersal centre on the Swan Hills could not have flowed across ice-free lowlands until after ~13.5 ka BP; similarly, ice on the Birch and Caribou Mountains and, Cameron and Clear Hills, could not have dispersed radially until after ~13 ka BP. Based on this evidence, these upland ice caps may have formed as a localized response to YD cooling.

6 Discussion

855 ### 6.1 Timing of ice sheet dynamic changes

Combining our ice dynamic reconstruction with existing chronologies, we reconstruct the behaviour of the SWLIS during the time period encompassing pre-LGM to the early Holocene. While switches in ice sheet dynamics and changes in ice-marginal behaviour have previously been recognized for the SWLIS (i.e., Ó Cofaigh et al., 2010; Ross et al., 2009; Margold et al., 2018; Evans et al., 2020), the duration over which these dynamic changes occurred and how they relate to climate forcing is less clear.

860

Integrating our flowset and ice-marginal geomorphic mapping with new deglacial chronologies, our reconstruction depicts three macroscale reorganizations of the ice drainage network followed by rapid ice sheet retreat and widespread stagnation that itself

Deleted: which is
Deleted: flow
Deleted: (Fig.
Deleted: nourished
Deleted: (non-ice streaming)
Deleted: recognise
Deleted: residual
Deleted: .,
Deleted: .
Deleted: descend
Deleted: crosscut
Deleted: were active after their surrounding lowlands were ice-free and that local ice-marginal lakes had drained prior to their advance
Deleted: cpas
Deleted: been invigorated
Deleted: pre-
Deleted: spanning
Deleted: , until now
Deleted: .

was punctuated by localized surging. These changes occurred over a ~2500 yr interval, synchronous with abrupt BA warming (14.7-12.9 ka BP). We, therefore, suggest that ice stream networks documented in the geomorphic record within the SWLIS evolved rapidly and were replaced by subsequent ice flows twice during this very short time period (see also Ross et al., 2009; Ó Cofaigh et al., 2010). During the LGM, the SWLIS drained via three large north-to-south oriented ice streams that were unconstrained by the regional topography. South-eastward flowing, topographically constrained ice streams later replaced these unconstrained ice streams during a macroscale switch in ice sheet dynamics. We suggest this switch from unconstrained to topographically constrained ice flows occurred contemporaneously with rapid ice sheet thinning at 14.9-14.3 ka BP (Stoker et al., 2022). South-eastward ice streaming would only have been sustained for a short period while the Plains Ice Divide remained active to support flow from the northwest to the southeast (Ross et al., 2009; Ó Cofaigh et al., 2010; Margold et al., 2015b, 2018). Following the formation of an 'ice-free corridor' between the CIS and LIS at 14.9 ka BP (Margold et al., 2019), south-eastward ice flows would have ceased (Ross et al., 2009; Ó Cofaigh et al., 2010; Margold et al., 2015b, 2018). In the central portions of the SWLIS, we observe widespread ice sheet downwasting and effective collapse associated with the shutdown of south-eastward flows and the isolation of this region. Within the northern portions of the SWLIS, south-eastward ice stream corridors were replaced by south-westward oriented ice streams (Ross et al., 2009; Ó Cofaigh et al., 2010; Margold et al., 2015b, 2018) that fed the rapidly retreating ice margin between 14.5-13 ka BP (Norris et al., 2022). As the ice margin reaches the Canadian Shield boundary at ~13 ka BP, we observe a ~1500 yr ice marginal standstill of the SWLIS. This standstill occurred contemporaneously with YD (12.9-11.7 ka BP) cooling (Norris et al., 2022).

6.2 Drivers of ice sheet dynamics

Comparing our reconstruction with climatic driving forces, macroscale reorganization and deglaciation of the SWLIS occurred synchronously with climatic warming during the BA interval. It is likely that ice sheet thinning during this interval would have exerted a major control on the SWLIS dynamics (Ross et al., 2009; Ó Cofaigh et al., 2010; Margold et al., 2015b, 2018). First, our reconstruction documents an initial switch in ice flow orientation from large topographically unconstrained ice streams that flowed north to south (CAIS, HPIS, Maskwa IS) to southeastward ice streaming (IS 2 complex), the orientation of which was controlled by the regional subglacial topography and fed by the Plains Ice Divide (Ross et al., 2009; Ó Cofaigh et al., 2010; Margold et al., 2015b, 2018). In agreement with previous work, we suggest that ice sheet thinning likely impeded north-to-south ice flow due to there being a lack of adequate ice thickness to sustain topographically unconstrained flows (Ross et al., 2009; Ó Cofaigh et al., 2010; Margold et al., 2015b, 2018). A second macroscale ice sheet reorganization within the northern portions of the SWLIS was characterized by a switch to southwestward ice streaming (Hay, Peace, and Athabasca river IS) (see also Ross et al., 2009; Margold et al., 2015b). We suggest this switch was driven by further ice sheet thinning (Ross et al., 2009), the shutdown of the Plains Ice Divide and the separation of the LIS and CIS (Margold et al., 2018). As the two ice sheets thinned and separated, there would have been inadequate ice input from the northwest to feed ice streaming to the southeast, and thus these ice flowpaths would have been replaced by ice streams that travelled through the Hay, Peace and Athabasca river lowlands fed solely by the Keewatin Ice Dome (Ross et al., 2009; Margold et al., 2015b, 2018).

In both cases, ice stream dynamics were likely driven by ice sheet thinning and changing ice divide configuration. However, these changes alone would not have caused these dramatic switches in ice stream orientation. Instead, these macroscale changes in ice sheet dynamics observed in the SWLIS are likely moderated by the region's subglacial topography (i.e., preglacial valley network). As the ice sheet thinned, the subglacial topography in the region ultimately controlled the direction of ice stream switching (Ross

et al., 2009; Ó Cofaigh et al., 2010). As such, this control, internal to the ice sheet system, influenced the wider response of the SWLIS to BA warming.

935 Our reconstruction also depicts a distinct change in the dynamics of the SWLIS during the YD. During this period of climatic cooling, we observe a slowdown in the ice sheet retreat rate and a widespread standstill of the SWLIS marked by the formation of the regionally extensive Cree Lake Moraine complex (Norris et al., 2022). At the same time, we record a switch from topographically constrained ice streaming in the Hay, Peace, Athabasca, and Churchill river lowlands to a regionally extensive and unconstrained sheet flow that fed the ice margin at its Cree Lake Moraine position. While it is highly likely that these dynamics 940 were influenced by the external climate forcing of the YD, the regions' underlying lithology and topography likely moderated the ice sheets' response to the external forcing (Margold et al., 2018). Interestingly, these changes in ice flow behaviour and regional ice margin standstill occur at the transition from the soft (deformable) sediment-covered Western Canadian Sedimentary Basin to the predominantly hard (rigid) bed of the crystalline Canadian Shield (Margold et al., 2018). While we acknowledge that in some areas, the Canadian Shield is mantled by sediment, the general change in the underlying bed composition (from predominantly soft 945 bedded to predominately hard bedded) likely resulted in an increase in bed strength and frictional resistance at the ice-bed interface, resulting in a decrease in ice velocity and, thus, potentially a slowing of the rate of ice sheet retreat perhaps even independent of external climate forcing (Bradwell et al., 2019). This pattern is analogous to changes observed in the northern portions of the British Irish Ice Sheet (Bradwell et al., 2019; Clark et al., 2022a), where bedrock lithology played a similar role in changing ice sheet dynamics. Furthermore, it is plausible that a shift from retreat down a reserve bed slope over the Western Canadian 950 Sedimentary Basin, with large time-transgressive ice-marginal glacial lakes (see Fig 6), to retreat across a normal bed slope, with less extensive impounded lakes on the Crystalline Shield also decreased retreat rates (e.g., Stokes and Clark, 2004; Evans et al., 2012; Utting and Atkinson, 2019). This was due to the changes in water availability at the ice-bed interface and the influence of this on ice dynamics (Carrivick and Tweed, 2013). The simultaneous change in lithology, bed slope, frequency of ice-marginal lakes and climate experienced by the SWLIS is in contrast to many other portions of the LIS at this time and may therefore help 955 explain why this sector of the LIS has such a marked response to YD cooling, especially in comparison to other portions of the western Laurentide margin (e.g., Gauthier et al., 2022; Reyes et al., 2022).

The dynamics we highlight above attest to the importance of considering glaciological, lithological and topographic factors in addition to external climate forcing when assessing ice sheet dynamic evolution over time. The interplay between internal and 960 external forcings of a terrestrial terminating has been highlighted for other ice sheets during the last glacial period (e.g., Landvik et al., 2014; Davies et al., 2019 see section 6.4), however, the changes in ice stream orientation, ice margin stagnation and localized surging highlighted in our reconstruction have not yet been well replicated by the existing numerical ice sheet reconstructions for the SWLIS (e.g., Tarasov et al., 2012). Quantifying and incorporating the effects of internal as well as external controls into numerical model reconstructions of the SWLIS should be a key area for future work to address.

965

6.3 The geomorphic imprint of abrupt climate change
In addition to the observed changes in ice flow direction, our geomorphic reconstruction also provides insight into the pattern and mechanism of ice recession. We observe a geomorphic imprint that signifies a period of active recession, widespread ice sheet stagnation punctuated by localized surging and then a return to widespread active recession (see Fig. 5 and 7). The spatial 970 variability in landforms diagnostic of these changes is best described as three zones. A southern 'Outer Deglacial Zone' encompasses the region between the LGM ice margin position and its retreat as far north as Red Deer (~52°N), an 'Intermediate

Deglacial Zone' encompasses the central regions of Alberta and Saskatchewan spanning from Red Deer to Cold Lake (~55°N) and an 'Inner Deglacial Zone' that spans the most northerly portion of the SWLIS and includes the region from Cold Lake to the Cree Lake Moraine complex. The juxtaposition of these three zones is likely the result of macroscale ice flow reorganizations that occurred during ice sheet thinning and deglaciation.

6.3.1 Outer Deglacial Zone

At the southern limits of the SWLIS, recessional push moraines are common across the landscape, most significantly the Lethbridge Moraine and the recessional moraines that reach the northern side of Cypress Hills (Westgate, 1968; Stalker, 1977; Kulig, 1996; Evans et al., 2008, 2012, 2014; Fig 5 and 6a). Multiple studies have invoked this landform signal to represent active recession of ice feeding the HPIS, CAIS, and Maskwa IS until they had retreated to the region north of Red Deer (Evans et al., 2008, 2014; Fig 4d). Outside of these ice stream tracks, active recession is marked by arcuate zones of 'aligned hummocks, ponds and ice-walled lake plains' (controlled moraine) diagnostic of warm and polythermal ice-marginal conditions (Evans et al., 2014; Fig. 3, 2020). This region also contains very limited glaciolacustrine sediments and landforms, which have previously been interpreted to be indicative of small, very short-lived proglacial lakes (Utting and Atkinson, 2019). We suggest this is the result of rapid active-ice sheet recession, which inhibited long-lived, widespread lake formation.

6.3.2 Intermediate Deglacial zone

The geomorphic record in central Alberta and Saskatchewan (i.e., north of Red Deer) contains a geomorphic record of widespread stagnation punctuated by localised surging (Fig. 5 and 7b). Within the ice stream central portions 'ice stream trunk zones' of the CAIS and Maskwa IS and the south-westward IS2 complex that crosses the region, ice sheet stagnation is demarcated by regions of well-preserved lineations (drumlinoid ridges and MSGL), which are overprinted by crevasse fill ridges (Ó Cofaigh et al., 2010). Bordering the flowpaths of these ice streams, large regions of inter-ice stream moraine containing hummocky terrain dominate the landscape (Evans et al., 2008, 2020). In some locations, glaciotectonic landforms, small localized moraines and streamlined zones that overprint the palaeo-ice stream imprint are interpreted as the product of local late-stage ice surging (Bretz, 1943; Evans, 2000; Evans et al., 2008; Ó Cofaigh et al., 2010; Evans et al., 2014, 2016; Atkinson et al., 2016; Evans et al., 2020). We suggest that local scale surging that punctuated widespread stagnation was most likely conditioned by the increased availability of subglacial meltwater and the development of local proglacial lakes around areas that contained downwasting ice (see also Evans et al., 2008, 2020).

We propose that the intermediate deglacial zone results from an 'ice sheet collapse' (ice sheet sector isolation, stagnation and downwasting) caused by ice stream switching and subsequent shutdown (Fig. 7b). This geomorphic signature was previously highlighted by Ó Cofaigh et al. (2010) and Ross et al. (2009) and we support the notion that this macroscale ice flow reorganization would have caused stagnation in higher topographic regions. These regions would have become separated from the ice sheet accumulation zone as ice flows shifted and began to flow in a southeast direction in topographically confined low-elevation areas (Ross et al., 2009; Ó Cofaigh et al., 2010). Following rapid ice sheet thinning, these southeast flowpaths would also have ceased, and ice would have downwasted, resulting in ice stagnation, including within the former ice stream flowpaths (Ross et al., 2009; Ó Cofaigh et al., 2010). In some locations, small local surge lobes would have occurred, overprinting the underlying geomorphology (Fig. 7c).

Although widespread ice sheet stagnation and downwasting (initial ice sheet collapse) would have been rapid, the landscape may have remained 'ice-cored' for several thousand years (Fig. 7c and d). In such regions, the thinning of the ice sheet would have allowed permafrost to aggrade beneath it and persist in the ice-cored terrain. Therefore, many regions of ice-cored hummocky terrain southwest of the Cree Lake Moraine, while formed during rapid ice downwasting, would have continued to be modified by the thawing of buried glacier ice into the Early Holocene. For example, in central Alberta in the Beaver Hills/ Cooking Lake region (20 km east of Edmonton), Emerson (1983) suggests glacial ice melt and permafrost thaw continued into the early Holocene and persisted until 9 ka BP based on radiocarbon ages from postglacial freshwater molluscs.

6.3.3 Inner Deglacial zone

Within the northern portions of Alberta and Saskatchewan, suites of moraines, eskers, and meltwater channels are visible within the Churchill, Athabasca and Peace river lowlands (Fig. 5 and 7c). These landforms document active retreat of the Hay, Peace and Athabasca River ice streams and IS 4/5 (Fig. 3b)(Margold et al., 2018, 2015b). In these regions, hummocky terrain is scarce and mostly restricted to upland regions (e.g., the Caribou and Birch Mountains and the Buffalo Head Hills) (see, Paulen and McClenaghan, 2015; Atkinson et al., 2018). Active ice retreat can be traced northeast, following the long axis of each valley as far north as the Canadian Shield boundary. The ice sheet retreat slowed to a standstill at this location to form the regionally extensive Cree Lake Moraine complex.

The marked change in deglacial behaviour observed across the SWLIS demonstrates the instability of a terrestrially terminating ice margin under rapid climatic warming. The behaviour of the 'Intermediate Deglacial Zone' was the result of macroscale ice stream reorganization that isolated a large portion of the SWLIS and forced an effective collapse in this region. This ice stream response was triggered by the rapid thinning of the CIS-LIS convergence zone, collapse of the CIS-LIS saddle and final shutdown of the Plains Ice Divide (Margold et al., 2018) and thus highlights how the ice sheet, through changes in the ice flow regime, can be highly sensitive to rapid climatic change. Although the response of the SWLIS to climatic change is complex, we suggest that its geomorphic imprint identified here is not unique and propose that the combination of regions of rapid ice marginal retreat and ice sheet disintegration and downwasting may be a valuable indicator of terrestrial ice sheet collapse, especially in soft-bedded regions.

6.4 Comparison to other ice sheets dynamics

The documented changes within the SWLIS provide valuable insight into the dynamics of ice streams in a region associated with a terrestrially terminating ice sheet margin during a period of rapid climate change. Despite its much larger scale, the behaviour of the SWLIS exhibits similarities to the deglacial changes observed within the interior portions of the last British Irish Ice Sheet (Greenwood and Clark, 2009; Davies et al., 2019; Clark et al., 2022a) and the (Late Weichselian) Svalbard-Barents Sea Ice Sheet (Landvik et al., 2014). These ice sheets exhibited relatively rapid, major changes in ice sheet and ice stream dynamics during a single glaciation. In all three cases, at the local last glacial maximum, the ice sheet dynamics were predominantly driven by changes in external climatic forcings, such as changes in global temperatures and regional precipitation patterns, and were less sensitive to internal controls, such as topography or lithological variations (Landvik et al., 2014; Davies et al., 2019). However, as noted by Davies et al. (2019) associated with a decrease in an ice sheets thickness, lithological and topographic controls start to play a more dominant role, modifying the macroscale changes in ice flow dynamics that were initially a response to the external climatic forcing. Based on our reconstruction of the SWLIS and the examples provided above, we suggest that while external climatic forcing is often implicated as a driver of change in ice sheet and ice stream dynamics at terrestrially terminating ice sheet margins,

such changes may not result implicitly from this control alone. Instead, the ice sheet dynamic result from a combination of external climatic forcing, as well as internal glaciological, lithological and topographic controls (Greenwood and Clark, 2009; Ross et al., 2009; Ó Cofaigh et al., 2010; Landvik et al., 2014; Margold et al., 2015b; Davies et al., 2019), and thus both should be considered.

7 Conclusion

Using glacial geomorphological inversion methods (flowsets) in combination with a recently compiled regional chronological synthesis, we reconstruct the ice flow and ice-marginal retreat dynamics of the SWLIS into five snapshots of ice sheet behaviour that encompass the time period from pre-LGM to the early Holocene. Our reconstruction shows ice stream behaviour comprising three macroscale reorganizations in the orientation and dynamics of ice streaming followed by regional deglaciation associated with a rapid increase in northern hemisphere temperatures during the BA. Early, faintly preserved, westward flows are documented, by a small number of flowsets and likely demarcate an early stage of ice streaming before the LGM. At the LGM our flowsets document the southward flow of the CAIS, HPIS and Maskwa Ice Stream. Linked to ice sheet thinning at ~15 ka, a macroscale reorganization in ice stream flow occurred, resulting in a series of southeastward flows. A second macroscale reorganization in ice flow is then observed at ~14 ka, where southwestern ice flow is restricted to the Hay, Peace, Athabasca, and Churchill river lowlands. During the YD, rates of ice sheet retreat then slowed. At this time, the ice sheet margin was located north of the Canadian Shield boundary and ice flow continued to be sourced from the northeast. Resulting from these phases of ice sheet dynamics we observe a three-part zonation of ice marginal geomorphology within the SWLIS, that demarcates active ice margin recession followed by punctuated ice sheet stagnation and downwasting (terrestrial ice sheet collapse). We attribute these macroscale changes in ice flow geometry and the associated deglacial behaviour to external climatic controls during the BA and YD. We also highlight the concordant role of internal (glaciological, lithological and topographic) controls in influencing how an ice sheet responds to external climate controls.

Data availability. The data referred to in this paper is provided within the tables and figures in the main text and in the supplementary materials related to this article are available in the Supplement and at https://figshare.com/s/4270b557926dd0806938. LiDAR DEMs were provided by the Government of Alberta (2017). LiDAR Data Archives. These data were provided under license and with project-specific data-sharing agreements by the Archaeological Survey of Alberta, Culture, Multiculturalism, and the Status of Women. Edmonton, Alberta via geodiscoveralberta@gov.ab.ca through https://geodiscover.alberta.ca/ geoportal/#searchPanel. SRTM DEMs were accessed via the USGS EROS Archive (EROS Centre, 2018) (https://www.usgs.gov/centers/eros/science/usgs-eros-archive-digital-elevation-shuttle-radar-topography-mission-srtm-non, last accessed Aug 15th 2023).

Supplement. The supplement related to this article is available online at: https://figshare.com/s/4270b557926dd0806938.

Author contributions. This project was conceptualized by DGF and SN with input from MM. Geomorphic mapping and flowset inventories were developed by SLN, NA and DJAE. The data visualization and figure creation were completed by SLN with input from all authors The manuscript was written by SLN with input from all authors.

Competing interests. The contact author has declared that none of the authors has any competing interests.

1185 **Acknowledgements.** We are grateful for comments and discussion from B. Menounos, J. England and A. Reyes on an early version of this manuscript. Internal reviews from M. Grobe and D. Utting at the Alberta Geological Survey helped clarify the manuscript. We thank reviewers Samuel Kelley and Isabelle McMartin for their helpful reviews that improve the quality of this paper.

Financial support. This research was funded by the Natural Sciences and Engineering Research Council and the Canada
1190 Research Chairs Program awarded to DGF, the Czech Science Foundation grant no. 19-21216Y awarded to MM, and grants from the University of Alberta Northern Research Awards to SLN.

References

Alley, R. B. and Bindschadler, R. A.: The West Antarctic Ice Sheet: behavior and environmentEdited by Richard B. Alley & Robert A. Bindschadler Antarctic Research Series volume 77, American Geophysical Union, Washington (2001). 294 pages. Price
1195 (65 AGU members 45.50). ISBN 0 87590957 4, Antarct. Sci., 13, 221–222, https://doi.org/10.1017/s0954102001220306, 2001.

Alley, R. B., Clark, P. U., Huybrechts, P., and Joughin, I.: Ice-sheet and sea-level changes, Science, 310, 456–460, https://doi.org/10.1126/science.1114613, 2005.

Anderson, T. W.: Evidence from Nipawin Bay in Frobisher Lake, Saskatchewan, for three highstand and three lowstand lake phases between 9 and 10 (10.1 and 11.5 cal) ka BP, Quat. Int., 260, 66–75, https://doi.org/10.1016/j.quaint.2011.09.021, 2012.

1200 Andriashek, L. D. and Atkinson, N.: Buried channels and glacial-drift aquifers in the Fort McMurray region, Northeast Alberta, Earth Sciences Report 2007-01, Alberta Geological Survey, Alberta Energy Utilities Board, 160, 2007.

Atkinson, Utting, and Pawley: An update to the glacial landforms map of Alberta, Alberta Geological Survey, 2018.

Atkinson, N.: Surficial Geology and Quaternary History of the High PrairieArea (NTS 83N/SE), 2009.

Atkinson, N. and Utting, D.: Glacial Flowlines of Alberta, 2021.

1205 Atkinson, N., Utting, D. J., and Pawley, S. M.: Glacial landforms of Alberta, Alberta Geological Survey, AER/AGS Map 604, 2014.

Atkinson, N., Pawley, S., and Utting, D. J.: Flow-pattern evolution of the Laurentide and Cordilleran ice sheets across west-central Alberta, Canada: implications for ice sheet growth, retreat and dynamics during the last glacial cycle, J. Quat. Sci., 31, 753–768, https://doi.org/10.1002/jqs.2901, 2016.

1210 Banks, J. and Harris, N. B.: Geothermal potential of Foreland Basins: A case study from the Western Canadian Sedimentary Basin, Geothermics, 76, 74–92, https://doi.org/10.1016/j.geothermics.2018.06.004, 2018.

Batchelor, C. L., Margold, M., Krapp, M., Murton, D. K., Dalton, A. S., Gibbard, P. L., Stokes, C. R., Murton, J. B., and Manica, A.: The configuration of Northern Hemisphere ice sheets through the Quaternary, Nat. Commun., 10, 3713, https://doi.org/10.1038/s41467-019-11601-2, 2019.

1215 Bednarski, J. M.: Surficial geology, Trutch, British Columbia (NTS 94G), Geological Survey of Canada, 2000.

Bradwell, T., Small, D., Fabel, D., Smedley, R. K., Clark, C. D., Saher, M. H., Callard, S. L., Chiverrell, R. C., Dove, D., Moreton, S. G., Roberts, D. H., Duller, G. A. T., and Ó Cofaigh, C.: Ice-stream demise dynamically conditioned by trough shape and bed strength, Sci. Adv., 5, eaau1380, https://doi.org/10.1126/sciadv.aau1380, 2019.

Breckenridge, A.: The Tintah-Campbell gap and implications for glacial Lake Agassiz drainage during the Younger Dryas cold
1220 interval, Quat. Sci. Rev., 117, 124–134, https://doi.org/10.1016/j.quascirev.2015.04.009, 2015.

Bretz, J. H.: Keewatin end moraines in Alberta, Canada, Geol. Soc. Am. Bull., 54, 31–52, https://doi.org/10.1130/gsab-54-31, 1943.

Carlson, A. E. and Clark, P. U.: Ice sheet sources of sea level rise and freshwater discharge during the last deglaciation, Rev. Geophys., 50, https://doi.org/10.1029/2011rg000371, 2012.

1225 Carrivick, J. L. and Tweed, F. S.: Proglacial lakes: character, behaviour and geological importance, Quat. Sci. Rev., 78, 34–52, https://doi.org/10.1016/j.quascirev.2013.07.028, 2013.

Christiansen, E. A.: The Wisconsinan deglaciation, of southern Saskatchewan and adjacent areas, Can. J. Earth Sci., 16, 913–938, https://doi.org/10.1139/e79-079, 1979.

Clark, C. D.: Glaciodynamic context of subglacial bedform generation and preservation, Ann. Glaciol., 28, 23–32,
1230 https://doi.org/10.3189/172756499781821832, 1999.

Clark, C. D., Ely, J. C., Hindmarsh, R. C. A., Bradley, S., Ignéczi, A., Fabel, D., Ó Cofaigh, C., Chiverrell, R. C., Scourse, J., Benetti, S., Bradwell, T., Evans, D. J. A., Roberts, D. H., Burke, M., Callard, S. L., Medialdea, A., Saher, M., Small, D., Smedley, R. K., Gasson, E., Gregoire, L., Gandy, N., Hughes, A. L. C., Ballantyne, C., Bateman, M. D., Bigg, G. R., Doole, J., Dove, D., Duller, G. A. T., Jenkins, G. T. H., Livingstone, S. L., McCarron, S., Moreton, S., Pollard, D., Praeg, D., Sejrup, H. P., Van
1235 Landeghem, K. J. J., and Wilson, P.: Growth and retreat of the last British–Irish Ice Sheet, 31 000 to 15 000 years ago: the BRITICE-CHRONO reconstruction, Boreas, 51, 699–758, https://doi.org/10.1111/bor.12594, 2022a.

Clark, J., Carlson, A. E., Reyes, A. V., Carlson, E. C. B., Guillaume, L., Milne, G. A., Tarasov, L., Caffee, M., Wilcken, K., and Rood, D. H.: The age of the opening of the Ice-Free Corridor and implications for the peopling of the Americas, Proc. Natl. Acad. Sci. U. S. A., 119, e2118558119, https://doi.org/10.1073/pnas.2118558119, 2022b.

1240 Clark, P. U.: Unstable behavior of the Laurentide ice sheet over deforming sediment and its implications for climate change, Quat. Res., 41, 19–25, https://doi.org/10.1006/qres.1994.1002, 1994.

Clark, P. U., Dyke, A. S., Shakun, J. D., Carlson, A. E., Clark, J., Wohlfarth, B., Mitrovica, J. X., Hostetler, S. W., and McCabe, A. M.: The Last Glacial Maximum, Science, 325, 710–714, https://doi.org/10.1126/science.1172873, 2009.

Clayton, L., Teller, J. T., and Attig, J. W.: Surging of the southwestern part of the Laurentide Ice Sheet, Boreas, 14, 235–241,
1245 https://doi.org/10.1111/j.1502-3885.1985.tb00726.x, 1985.

Cummings, D. I., Russell, H. A. J., and Sharpe, D. R.: Buried valleys and till in the Canadian Prairies: geology, hydrogeology, and origin. Geological Survey of Canada, 2012.

Dalton, A. S., Margold, M., Stokes, C. R., and Tarasov, L.: An updated radiocarbon-based ice margin chronology for the last deglaciation of the North American Ice Sheet Complex, Quat. Sci. Rev., 2020.

1250 Dalton, A. S., Stokes, C. R., and Batchelor, C. L.: Evolution of the Laurentide and Innuitian ice sheets prior to the Last Glacial Maximum (115 ka to 25 ka), Earth-Sci. Rev., 224, 103875, https://doi.org/10.1016/j.earscirev.2021.103875, 2022.

Davies, B. J., Livingstone, S. J., Roberts, D. H., Evans, D. J. A., Gheorghiu, D. M., and Ó Cofaigh, C.: Dynamic ice stream retreat in the central sector of the last British-Irish Ice Sheet, Quat. Sci. Rev., 225, 105989, https://doi.org/10.1016/j.quascirev.2019.105989, 2019.

1255 De Angelis, H. and Kleman, J.: Palaeo-ice-stream onsets: examples from the north-eastern Laurentide Ice Sheet, Earth Surf. Process., 33, 560–572, https://doi.org/10.1002/esp.1663, 2008.

Dyke, A. S.: An outline of North American deglaciation with emphasis on central and northern Canada, in: Quaternary Glaciations-Extent and Chronology - Part II: North America, Elsevier, 373–424, https://doi.org/10.1016/s1571-0866(04)80209-4, 2004.

Dyke, A. S. and Prest, V. K.: Late Wisconsinan and Holocene history of the Laurentide Ice Sheet, Géogr. phys. quat., 41, 237–
1260 263, https://doi.org/10.7202/032681ar, 1987.

Dyke, A. S., Andrews, J. T., Clark, P. U., England, J. H., Miller, G. H., Shaw, J., and Veillette, J. J.: The Laurentide and Innuitian ice sheets during the Last Glacial Maximum, Quat. Sci. Rev., 21, 9–31, https://doi.org/10.1016/s0277-3791(01)00095-6, 2002.

Emerson, D.: Late glacial molluscs from the Cooking Lake moraine, Alberta, Canada, Can. J. Earth Sci., 20, 160–162, https://doi.org/10.1139/e83-014, 1983.

1265 EROS Centre: USGS EROS Archive – Digital Elevation – Shuttle Radar Topography Mission (SRTM) 1 Arc-Second Global, https://doi.org/10.5066/F7PR7TFT, 2018.

Evans, D. J. A.: Quaternary geology and geomorphology of the Dinosaur Provincial Park area and surrounding plains, Alberta, Canada: the identification of former glacial lobes, drainage diversions and meltwater flood tracks, Quat. Sci. Rev., 19, 931–958, https://doi.org/10.1016/s0277-3791(99)00029-3, 2000.

1270 Evans, D. J. A.: Glacial Landsystems, in: Glacier Science and Environmental Change, Blackwell Publishing, Malden, MA, USA, 83–88, https://doi.org/10.1002/9780470750636.ch18, 2007.

Evans, D. J. A.: GLACIAL LANDFORMS | Glacial Landsystems, in: Encyclopedia of Quaternary Science, Elsevier, 813–824, https://doi.org/10.1016/b978-0-444-53643-3.00069-8, 2013.

Evans, D. J. A. and Campbell, I. A.: Quaternary stratigraphy of the buried valleys of the lower Red Deer River, Alberta, Canada, 1275 J. Quat. Sci., 10, 123–148, https://doi.org/10.1002/jqs.3390100204, 1995.

Evans, D. J. A., Lemmen, D. S., and Rea, B. R.: Glacial landsystems of the southwest Laurentide Ice Sheet: modern Icelandic analogues, J. Quat. Sci., 14, 673–691, https://doi.org/10.1002/(sici)1099-1417(199912)14:7<673::aid-jqs467>3.0.co;2-#, 1999.

Evans, D. J. A., Clark, C. D., and Rea, B. R.: Landform and sediment imprints of fast glacier flow in the southwest Laurentide Ice Sheet, J. Quat. Sci., 23, 249–272, https://doi.org/10.1002/jqs.1141, 2008.

1280 Evans, D. J. A., Hiemstra, J. F., Boston, C. M., Leighton, I., Cofaigh, C. Ó., and Rea, B. R.: Till stratigraphy and sedimentology at the margins of terrestrially terminating ice streams: case study of the western Canadian prairies and high plains, Quat. Sci. Rev., 46, 80–125, https://doi.org/10.1016/j.quascirev.2012.04.028, 2012.

Evans, D. J. A., Young, N. J. P., and Ó Cofaigh, C.: Glacial geomorphology of terrestrial-terminating fast flow lobes/ice stream margins in the southwest Laurentide Ice Sheet, Geomorphology (Amst.), 204, 86–113, 1285 https://doi.org/10.1016/j.geomorph.2013.07.031, 2014.

Evans, D. J. A., Storrar, R. D., and Rea, B. R.: Crevasse-squeeze ridge corridors: Diagnostic features of late-stage palaeo-ice stream activity, Geomorphology , 258, 40–50, https://doi.org/10.1016/j.geomorph.2016.01.017, 2016.

Evans, D. J. A., Atkinson, N., and Phillips, E.: Glacial geomorphology of the Neutral Hills Uplands, southeast Alberta, Canada: The process-form imprints of dynamic ice streams and surging ice lobes, Geomorphology (Amst.), 350, 106910, 1290 https://doi.org/10.1016/j.geomorph.2019.106910, 2020.

Evans, D. J. A., Phillips, E. R., and Atkinson, N.: Glacitectonic rafts and their role in the generation of Quaternary subglacial bedforms and deposits, Quat. Res., 104, 101–135, https://doi.org/10.1017/qua.2021.11, 2021.

Eyles, N., Boyce, J. I., and Barendregt, R. W.: Hummocky moraine: sedimentary record of stagnant Laurentide Ice Sheet lobes resting on soft beds, Sediment. Geol., 123, 163–174, https://doi.org/10.1016/s0037-0738(98)00129-8, 1999.

1295 Fenton, M. M., Waters, E. J., Pawley, S. M., Atkinson, N., Utting, D. J., and McKay, K.: Surficial geology of Alberta. Alberta Geological Survey, Alberta Geological Survey, AER/AGS Map 601, 2013.

Fisher, T. G. and Smith, D. G.: Glacial Lake Agassiz: Its northwest maximum extent and outlet in Saskatchewan (Emerson Phase), Quat. Sci. Rev., 13, 845–858, https://doi.org/10.1016/0277-3791(94)90005-1, 1994.

Fisher, T. G., Waterson, N., Lowell, T. V., and Hajdas, I.: Deglaciation ages and meltwater routing in the Fort McMurray region, 1300 northeastern Alberta and northwestern Saskatchewan, Canada, Quat. Sci. Rev., 28, 1608–1624, https://doi.org/10.1016/j.quascirev.2009.02.003, 2009.

Froese, D. F., Young, J. M., Norris, S. L., and Margold, M.: Availability and viability of the ice-free corridor and pacific coast routes for the peopling of the Americas, SAA Archaeological Record, 2019.

Gauthier, M. S., Breckenridge, A., and Hodder, T. J.: Patterns of ice recession and ice stream activity for the MIS 2 Laurentide Ice 1305 Sheet in Manitoba, Canada, Boreas, 51, 274–298, https://doi.org/10.1111/bor.12571, 2022.

Geological Survey of Canada: Surficial geology of Canada / Géologie des formations superficielles du Canada, Natural Resources Canada, https://doi.org/10.4095/295462, 2014.

Gowan, E. J., Tregoning, P., Purcell, A., Montillet, J.-P., and McClusky, S.: A model of the western Laurentide Ice Sheet, using observations of glacial isostatic adjustment, Quat. Sci. Rev., 139, 1–16, https://doi.org/10.1016/j.quascirev.2016.03.003, 2016.

1310 Greenwood, S. L. and Clark, C. D.: Reconstructing the last Irish Ice Sheet 1: changing flow geometries and ice flow dynamics deciphered from the glacial landform record, Quat. Sci. Rev., 28, 3085–3100, https://doi.org/10.1016/j.quascirev.2009.09.008, 2009.

Greenwood, S. L., Clark, C. D., and Hughes, A. L. C.: Formalising an inversion methodology for reconstructing ice-sheet retreat patterns from meltwater channels: application to the British Ice Sheet, J. Quat. Sci., 22, 637–645, https://doi.org/10.1002/jqs.1083, 1315 2007.

Gregoire, L. J., Otto-Bliesner, B., Valdes, P. J., and Ivanovic, R.: Abrupt Bølling warming and ice saddle collapse contributions to the Meltwater Pulse 1a rapid sea level rise, Geophys. Res. Lett., 43, 9130–9137, https://doi.org/10.1002/2016GL070356, 2016.

GSC: Geoscience Data Repository. Natural Resources Canada, Ottawa, 2008.

Heintzman, P. D., Froese, D., Ives, J. W., Soares, A. E. R., Zazula, G. D., Letts, B., Andrews, T. D., Driver, J. C., Hall, E., Hare, 1320 P. G., Jass, C. N., MacKay, G., Southon, J. R., Stiller, M., Woywitka, R., Suchard, M. A., and Shapiro, B.: Bison phylogeography constrains dispersal and viability of the Ice Free Corridor in western Canada, Proc. Natl. Acad. Sci. U. S. A., 113, 8057–8063, https://doi.org/10.1073/pnas.1601077113, 2016.

Hickin, A. S. and Fournier, M. A.: Compilation of Geological Survey of Canada surficial geology maps for NTS 94A and 93P, British Columbia Ministry of Energy, Mines and Petroleum Resources, British Columbia Geological Survey Open File 2011-02; 1325 Geoscience BC Map, 1:250,000 scale, 2011.

Horberg, L.: Pleistocene drift sheets in the Lethbridge region, Alberta, Canada, J. Geol., 60, 303–330, https://doi.org/10.1086/625981, 1952.

Hughes, A. L. C., Clark, C. D., and Jordan, C. J.: Flow-pattern evolution of the last British Ice Sheet, Quat. Sci. Rev., 89, 148–168, https://doi.org/10.1016/j.quascirev.2014.02.002, 2014.

1330 Klassen, R. W.: Quaternary geology of the southern Canadian in- terior plains, in: Quaternary Geology of Canada and Greenland, edited by: Fulton, R. J., Geological Society of America, Boulder, CO, 138–174, 1989.

Klassen, R. W.: Late Wisconsinan and Holocene history of southwestern Saskatchewan, Can. J. Earth Sci., 31, 1822–1837, https://doi.org/10.1139/e94-162, 1994.

Kleman, J. and Borgström, I.: Reconstruction of palaeo-ice sheets: The use of geomorphological data, Earth Surf. Process., 21, 1335 893–909, https://doi.org/10.1002/(sici)1096-9837(199610)21:10<893::aid-esp620>3.0.co;2-u, 1996.

Kleman, J., Hättestrand, C., Borgström, I., and Stroeven, A.: Fennoscandian palaeoglaciology reconstructed using a glacial geological inversion model, J. Glaciol., 43, 283–299, https://doi.org/10.1017/s0022143000003233, 1997.

Kleman, J., Httestrand, C., Stroeven, A. P., Jansson, K. N., De Angelis, H., and Borgstrm, I.: Reconstruction of palaeo-ice sheets - inversion of their glacial geomorphological record, in: Glacier Science and Environmental Change, Blackwell Publishing, 1340 Malden, MA, USA, 192–198, https://doi.org/10.1002/9780470750636.ch38, 2006.

Kleman, J., Jansson, K., De Angelis, H., Stroeven, A. P., Hättestrand, C., Alm, G., and Glasser, N.: North American Ice Sheet build-up during the last glacial cycle, 115–21kyr, Quat. Sci. Rev., 29, 2036–2051, https://doi.org/10.1016/j.quascirev.2010.04.021, 2010.

Kulig, J. J.: The glaciation of the Cypress Hills of Alberta and Saskatchewan and its regional implications, Quat. Int., 32, 53–77, 1345 https://doi.org/10.1016/1040-6182(95)00059-3, 1996.

Lambeck, K., Purcell, A., and Zhao, S.: The North American Late Wisconsin ice sheet and mantle viscosity from glacial rebound analyses, Quat. Sci. Rev., 158, 172–210, https://doi.org/10.1016/j.quascirev.2016.11.033, 2017.

Landvik, J. Y., Alexanderson, H., Henriksen, M., and Ingólfsson, Ó.: Landscape imprints of changing glacial regimes during ice-sheet build-up and decay: a conceptual model from Svalbard, Quat. Sci. Rev., 92, 258–268, 1350 https://doi.org/10.1016/j.quascirev.2013.11.023, 2014.

Leckie, D. A.: Tertiary fluvial gravels and evolution of the Western Canadian Prairie Landscape, Sediment. Geol., 190, 139–158, https://doi.org/10.1016/j.sedgeo.2006.05.019, 2006.

Lemmen, D. S., Duk-Rodkin, A., and Bednarski, J. M.: Late glacial drainage systems along the northwestern margin of the Laurentide Ice Sheet, Quat. Sci. Rev., 13, 805–828, https://doi.org/10.1016/0277-3791(94)90003-5, 1994.

1355 Margold, M., Stokes, C. R., Clark, C. D., and Kleman, J.: Ice streams in the Laurentide Ice Sheet: a new mapping inventory, J. Maps, 11, 380–395, https://doi.org/10.1080/17445647.2014.912036, 2015a.

Margold, M., Stokes, C. R., and Clark, C. D.: Ice streams in the Laurentide Ice Sheet: Identification, characteristics and comparison to modern ice sheets, Earth-Sci. Rev., 2015b.

Margold, M., Stokes, C. R., and Clark, C. D.: Reconciling records of ice streaming and ice margin retreat to produce a 1360 palaeogeographic reconstruction of the deglaciation of the Laurentide Ice Sheet, Quat. Sci. Rev., 2018.

Margold, M., Gosse, J. C., Hidy, A. J., Woywitka, R. J., Young, J. M., and Froese, D.: Beryllium-10 dating of the Foothills Erratics Train in Alberta, Canada, indicates detachment of the Laurentide Ice Sheet from the Rocky Mountains at ~15 ka, Quat. Res., 92, 469–482, https://doi.org/10.1017/qua.2019.10, 2019.

Mathews, W. H., Gabrielse, H., and Rutter, N. W.: Glacial maps of Beatton river map area, BritishColumbia. Geological Survey 1365 of Canada, Geological Survey of Canada, open file 274, 1:1,000,000 scale, 1975.

Mossop, G. D. and Shetsen, I.: Geological atlas of the Western Canada Sedimentary Basin; Canadian Society of Petroleum Geologists, Canadian Society of Petroleum Geologists and Alberta Research Council, 2012.

Munyikwa, K., Feathers, J. K., Rittenour, T. M., and Shrimpton, H. K.: Constraining the Late Wisconsinan retreat of the Laurentide ice sheet from western Canada using luminescence ages from postglacial aeolian dunes, Quat. Geochronol., 6, 407–422, 1370 https://doi.org/10.1016/j.quageo.2011.03.010, 2011.

Munyikwa, K., Rittenour, T. M., and Feathers, J. K.: Temporal constraints for the Late Wisconsinan deglaciation of western Canada using eolian dune luminescence chronologies from Alberta, Palaeogeogr. Palaeoclimatol. Palaeoecol., 470, 147–165, https://doi.org/10.1016/j.palaeo.2016.12.034, 2017.

Murton, J. B., Bateman, M. D., Dallimore, S. R., Teller, J. T., and Yang, Z.: Identification of Younger Dryas outburst flood path 1375 from Lake Agassiz to the Arctic Ocean, Nature, 464, 740–743, https://doi.org/10.1038/nature08954, 2010.

Norris, S., Tarasov, L., Monteath, A. J., Gosse, J. C., Hidy, A. J., Margold, M., and Froese, D. G.: Rapid retreat of the southwestern Laurentide Ice Sheet during the Bølling-Allerød interval, Geology, https://doi.org/10.1130/g49493.1, 2022.

Norris, S. L.: Glacial Flowlines in the Lower Athabasca and Clearwater Region Alberta and Saskatchewan, 2019.

Norris, S. L., Margold, M., and Froese, D. G.: Glacial landforms of northwest Saskatchewan, J. Maps, 2017.

1380 Norris, S. L., Garcia-Castellanos, D., Jansen, J. D., Carling, P. A., Margold, M., Woywitka, R. J., and Froese, D. G.: Catastrophic drainage from the northwestern outlet of glacial Lake Agassiz during the Younger Dryas, Geophysical, 2021.

Ó Cofaigh, C., Evans, D. J. A., and Smith, I. R.: Large-scale reorganization and sedimentation of terrestrial ice streams during late Wisconsinan Laurentide Ice Sheet deglaciation, Geol. Soc. Am. Bull., 122, 743–756, https://doi.org/10.1130/b26476.1, 2010.

Pattyn, F., Ritz, C., Hanna, E., Asay-Davis, X., DeConto, R., Durand, G., Favier, L., Fettweis, X., Goelzer, H., Golledge, N. R., 1385 Kuipers Munneke, P., Lenaerts, J. T. M., Nowicki, S., Payne, A. J., Robinson, A., Seroussi, H., Trusel, L. D., and van den Broeke, M.: The Greenland and Antarctic ice sheets under 1.5 °C global warming, Nat. Clim. Chang., 8, 1053–1061, https://doi.org/10.1038/s41558-018-0305-8, 2018.

Paulen, R. C. and McClenaghan, M. B.: Late Wisconsin ice-flow history in the Buffalo Head Hills kimberlite field, north-central Alberta, Can. J. Earth Sci., 52, 51–67, https://doi.org/10.1139/cjes-2014-0109, 2015.

1390 Pawluk, S. and Bayrock, L. A.: Some characteristics and physical properties of Alberta tills, Research Council of Alberta, 1969.

Peltier, W. R., Argus, D. F., and Drummond, R.: Space geodesy constrains ice age terminal deglaciation: The global ICE-6G_C (VM5a) model, Journal of Geophysical Research: Solid Earth, 120, 450–487, 2015.

Prest, V. K.: Nomenclature of moraines and ice-flow features as applied to the glacial map of Canada, Department of Energy, Mines and Resources, 1968.

1395 Prest, V. K., Grant, D. R., and Rampton, V. N.: Glacial Map of Canada, in: Geological Survey of Canada, Ottawa, 1968.

Rasmussen, S. O., Bigler, M., Blockley, S. P., Blunier, T., Buchardt, S. L., Clausen, H. B., Cvijanovic, I., Dahl-Jensen, D., Johnsen, S. J., Fischer, H., Gkinis, V., Guillevic, M., Hoek, W. Z., Lowe, J. J., Pedro, J. B., Popp, T., Seierstad, I. K., Steffensen, J. P., Svensson, A. M., Vallelonga, P., Vinther, B. M., Walker, M. J. C., Wheatley, J. J., and Winstrup, M.: A stratigraphic framework for abrupt climatic changes during the Last Glacial period based on three synchronized Greenland ice-core records: refining and extending the INTIMATE event stratigraphy, Quat. Sci. Rev., 106, 14–28, https://doi.org/10.1016/j.quascirev.2014.09.007, 2014.

Reyes, A. V., Carlson, A. E., Milne, G. A., Tarasov, L., Reimink, J. R., and Caffee, M. W.: Revised chronology of northwest Laurentide ice-sheet deglaciation from 10Be exposure ages on boulder erratics, Quat. Sci. Rev., 277, 107369, https://doi.org/10.1016/j.quascirev.2021.107369, 2022.

Rignot, E. and Kanagaratnam, P.: Changes in the velocity structure of the Greenland Ice Sheet, Science, 311, 986–990, https://doi.org/10.1126/science.1121381, 2006.

Rignot, E. and Thomas, R. H.: Mass balance of polar ice sheets, Science, 297, 1502–1506, https://doi.org/10.1126/science.1073888, 2002.

Rignot, E., Bamber, J. L., van den Broeke, M. R., Davis, C., Li, Y., van de Berg, W. J., and van Meijgaard, E.: Recent Antarctic ice mass loss from radar interferometry and regional climate modelling, Nat. Geosci., 1, 106–110, https://doi.org/10.1038/ngeo102, 2008.

Rignot, E., Velicogna, I., van den Broeke, M. R., Monaghan, A., and Lenaerts, J. T. M.: Acceleration of the contribution of the Greenland and Antarctic ice sheets to sea level rise, Geophys. Res. Lett., 38, https://doi.org/10.1029/2011gl046583, 2011.

Ross, M., Campbell, J. E., Parent, M., and Adams, R. S.: Palaeo-ice streams and the subglacial landscape mosaic of the North American mid-continental prairies, Boreas, 38, 421–439, https://doi.org/10.1111/j.1502-3885.2009.00082.x, 2009.

Sharp, M.: "crevasse-fill" ridges—A landform type characteristic of surging glaciers?, Geogr. Ann. Ser. A. Phys. Geogr., 67, 213–220, https://doi.org/10.1080/04353676.1985.11880147, 1985.

Shepherd, A.: Mass balance of the Antarctic Ice Sheet from 1992 to 2017, Nature, 556, 219–222, 2018.

Shetsen, I.: Application of till pebble lithology to the differentiation of glacial lobes in southern Alberta, Can. J. Earth Sci., 21, 920–933, https://doi.org/10.1139/e84-097, 1984.

Simpson, M. A.: Surficial geology map of Saskatchewan; Sask. Energy Mines/Sask. Resear. Counc., 1:1 000 000 scale, 1997.

Stalker, A. M.: Buried valleys in cetnral and southern Alberta, Geological Survey of Canada Paper, 1961.

Stalker, A. M.: Surficial geology, Lethbridge (east half), Geoglogical Survey of Canada, Ottawa, 1962.

Stalker, A. M.: Indications of Wisconsin and earlier man from the southwest Canadian prairies, Ann. N. Y. Acad. Sci., 288, 119–136, https://doi.org/10.1111/j.1749-6632.1977.tb33606.x, 1977.

Stoker, B. J., Margold, M., Gosse, J. C., Hidy, A. J., Monteath, A. J., Young, J. M., Gandy, N., Gregoire, L. J., Norris, S. L., and Froese, D.: The collapse of the Laurentide-Cordilleran ice saddle and early opening of the Mackenzie Valley, Northwest Territories, constrained by [10]Be exposure dating, , https://doi.org/10.5194/tc-2022-120, 2022.

Stokes, C. and Clark, C.: Evolution of late glacial ice-marginal lakes on the northwestern Canadian Shield and their influence on the location of the Dubawnt Lake palaeo-ice stream, Palaeogeogr. Palaeoclimatol. Palaeoecol., 215, 155–171, https://doi.org/10.1016/s0031-0182(04)00467-5, 2004.

Stokes, C. R. and Clark, C. D.: Geomorphological criteria for identifying Pleistocene ice streams, Ann. Glaciol., 28, 67–74, https://doi.org/10.3189/172756499781821625, 1999.

Stokes, C. R., Margold, M., Clark, C. D., and Tarasov, L.: Ice stream activity scaled to ice sheet volume during Laurentide Ice Sheet deglaciation, Nature, 530, 322–326, https://doi.org/10.1038/nature16947, 2016.

Tarasov, L., Dyke, A. S., Neal, R. M., and Peltier, W. R.: A data-calibrated distribution of deglacial chronologies for the North American ice complex from glaciological modeling, Earth Planet. Sci. Lett., 315–316, 30–40, https://doi.org/10.1016/j.epsl.2011.09.010, 2012.

Utting, D. J. and Atkinson, N.: Proglacial lakes and the retreat pattern of the southwest Laurentide Ice Sheet across Alberta, Canada, Quat. Sci. Rev., 2019.

1440   Utting, D. J., Atkinson, N., Pawley, S., and Livingstone, S. J.: Reconstructing the confluence zone between Laurentide and Cordilleran ice sheets along the Rocky Mountain Foothills, south-west Alberta, J. Quat. Sci., 31, 769–787, https://doi.org/10.1002/jqs.2903, 2016.

Westgate, J. A.: Surficial geology of the Foremost-Cypress Hills region, Alberta, 1968.

Woywitka, R.: Geoarchaeology of the mineable oil sands region, Northeastern Alberta, Canada, 2019.

1445   Young, J. M., Reyes, A. V., and Froese, D. G.: Assessing the ages of the Moorhead and Emerson phases of glacial Lake Agassiz and their temporal connection to the Younger Dryas cold reversal, Quat. Sci. Rev., 251, 106714, https://doi.org/10.1016/j.quascirev.2020.106714, 2021.

Young, R. R., Burns, J. A., Smith, D. G., Arnold, L. D., and Rains, R. B.: A single, late Wisconsin, Laurentide glaciation, Edmonton area and southwestern Alberta, Geology, 22, 683, https://doi.org/10.1130/0091-7613(1994)022<0683:aslwlg>2.3.co;2, 1994.

1450

1455
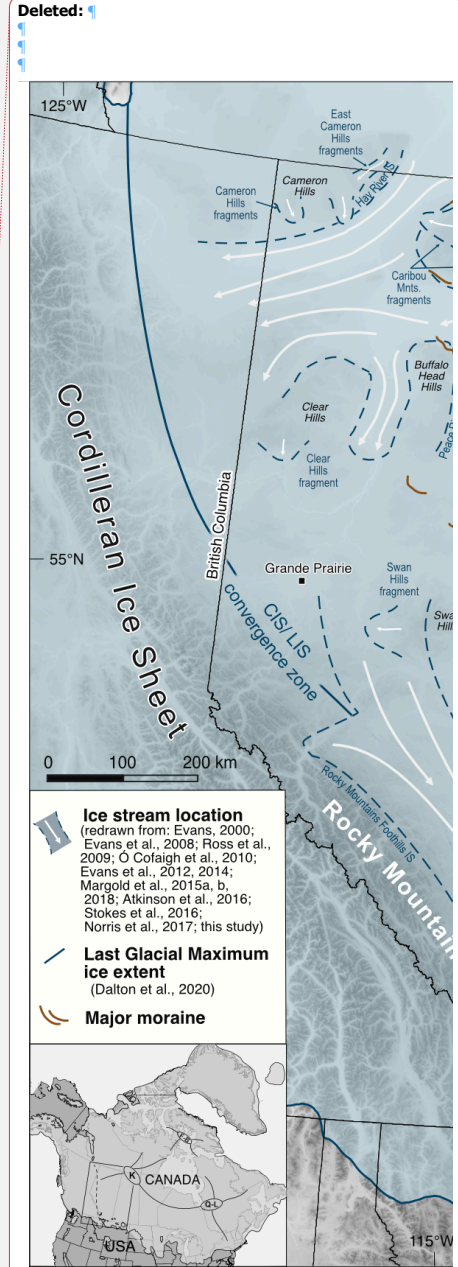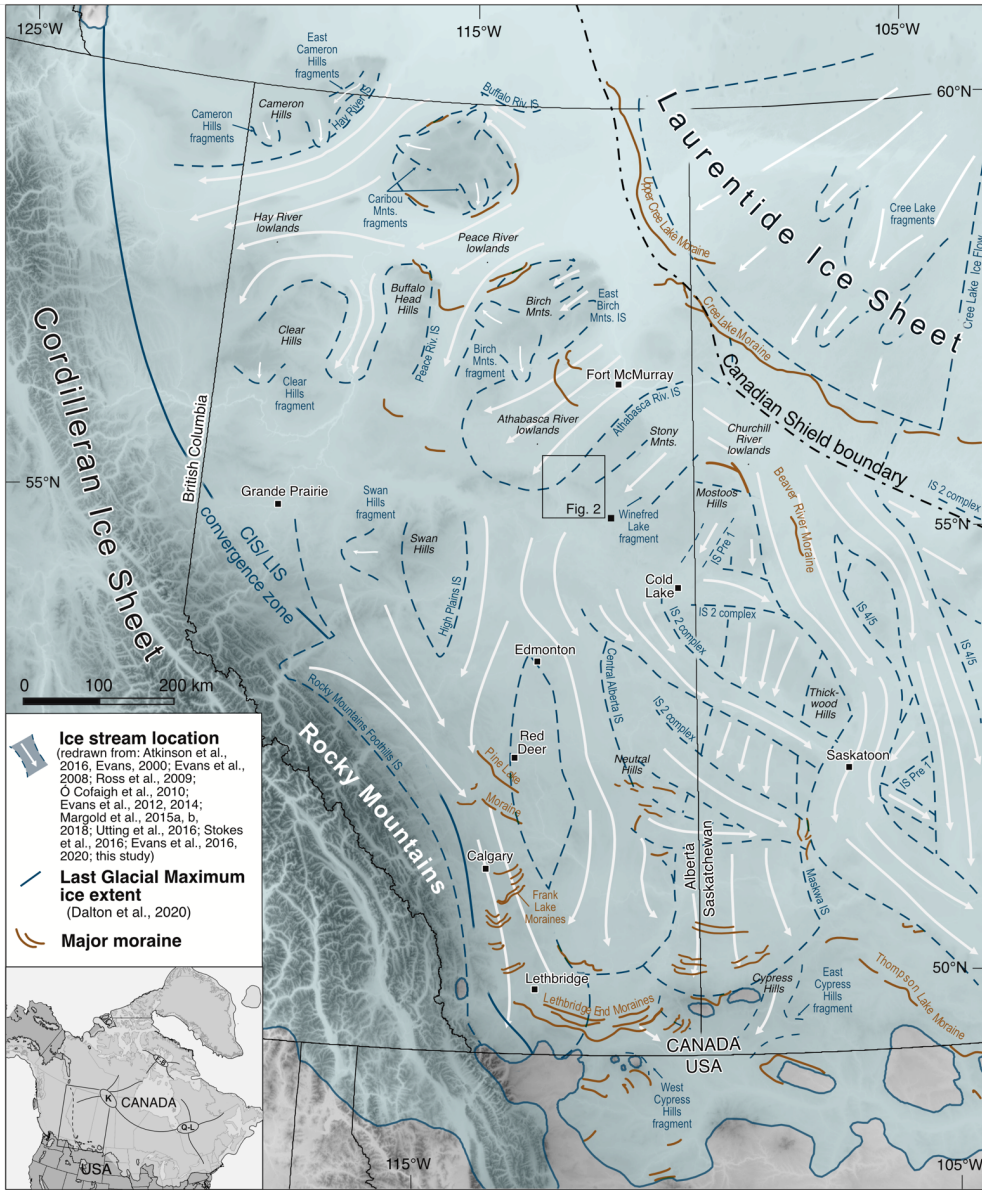
Figure 1: Regional ice-flow imprint of the southwestern sector of the Laurentide Ice Sheet. Digital elevation model (DEM) from the Shuttle Radar Topographic Mission (SRTM) provided by the USGS EROS Archive (EROS Centre, 2018). Last glacial maximum ice extent from Dalton et al. (2020).

1470

Deleted:
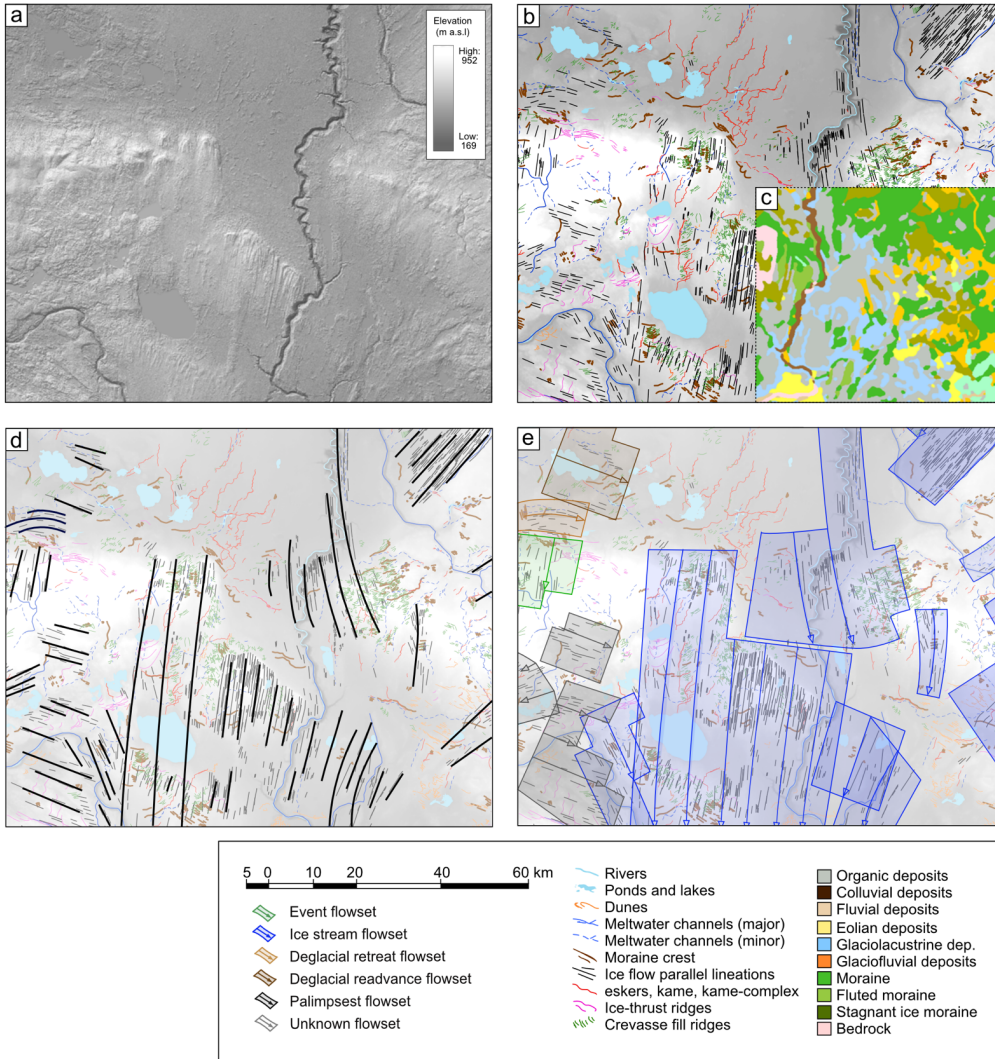
Figure 2: Classification of glacial geomorphology into flowsets. (a) Shuttle Radar Topography Mission (SRTM) imagery displaying the onset zone of the Central Alberta Ice Stream. (b) Area of corresponding geomorphological mapping (Atkinson et
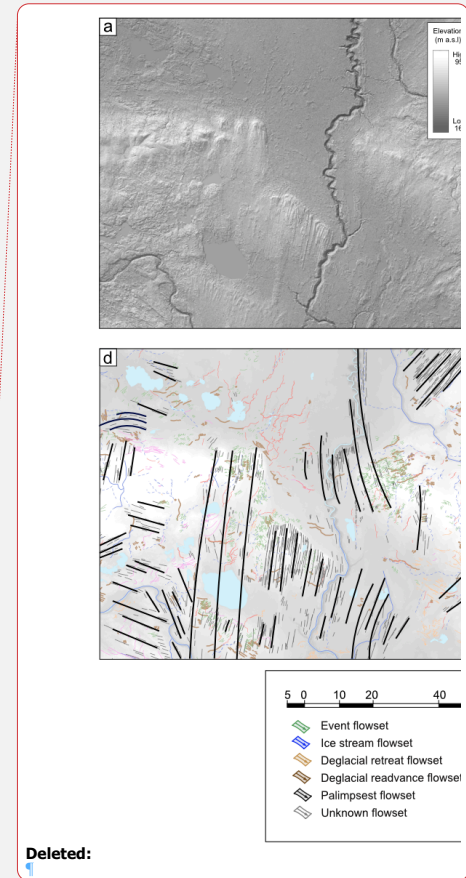
al., 2018) and, (c) surficial geological units (Fenton et al., 2013) (d). Simplification of geomorphic mapping and surficial geological units into 'flowlines' (e) Classification of flowlines into individual flowsets as either 'ice stream', 'deglacial retreat', "deglacial readvance' 'event' 'palimpsest' or 'unknown. See Figure 1 for the location of Figure 2 panel. Digital elevation model (DEM) from the Shuttle Radar Topographic Mission (SRTM) provided by the USGS EROS Archive (EROS Centre, 2018).
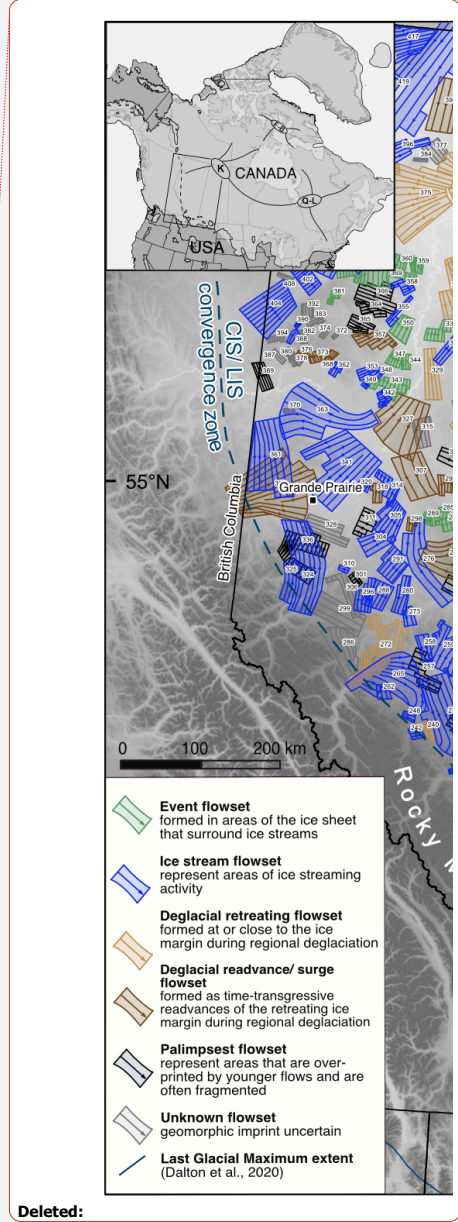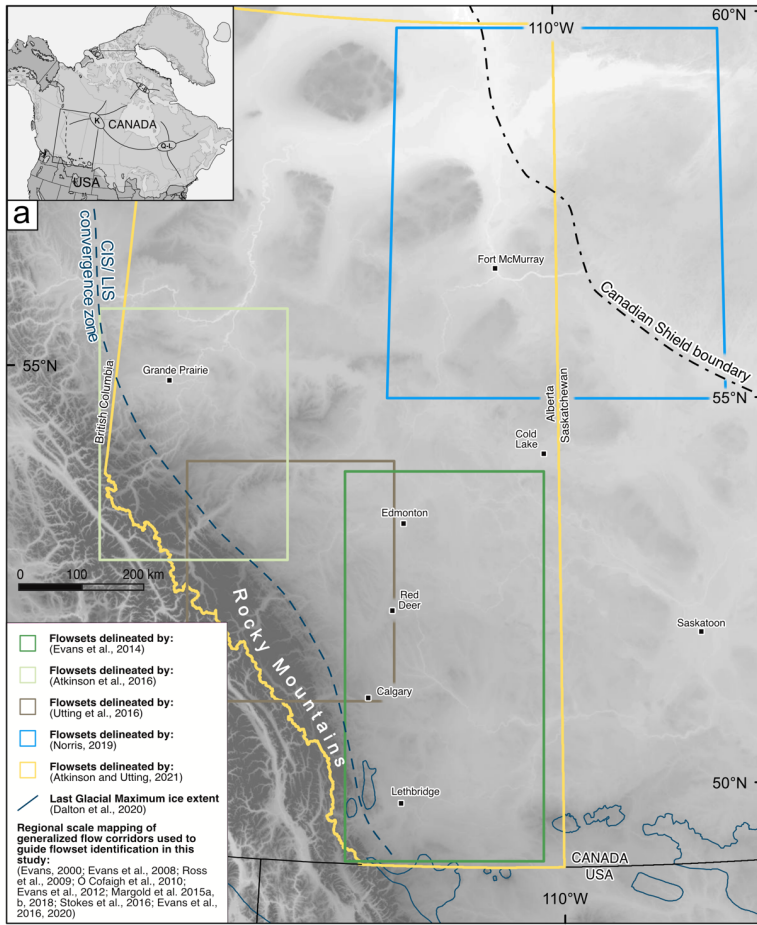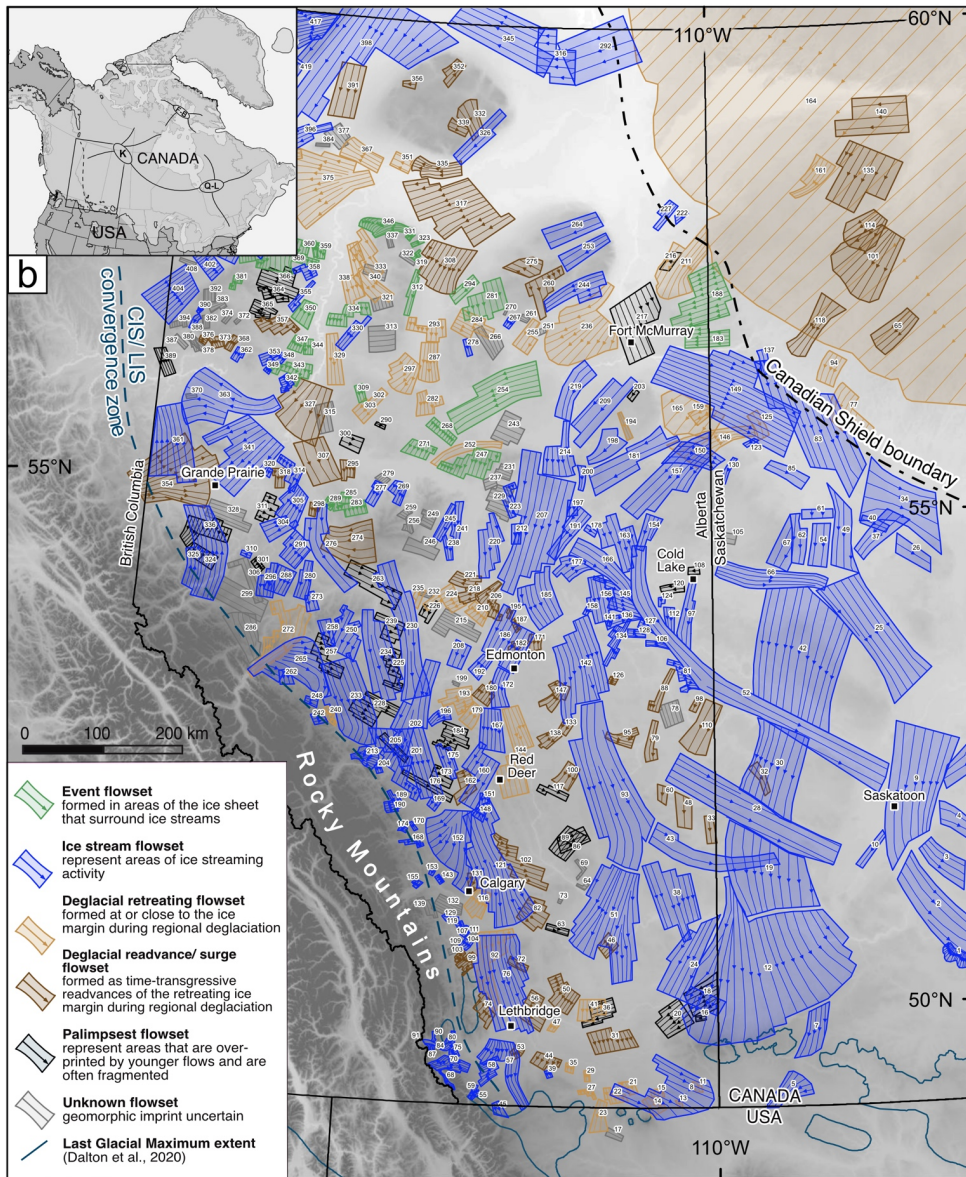
Figure 3: (a) Location of previous flowset mapping. (b) Flowset map of the southwestern Laurentide Ice Sheet (available as a supplementary .kml file). Flowset configuration reflects a highly dynamic system of fast flow caused by multiple reconfigurations in ice sheet drainage. Digital

1485

elevation model (DEM) from the Shuttle Radar Topographic Mission (SRTM) provided by the USGS EROS Archive (EROS Centre, 2018). Last glacial maximum ice extent from Dalton et al. (2020).

1490
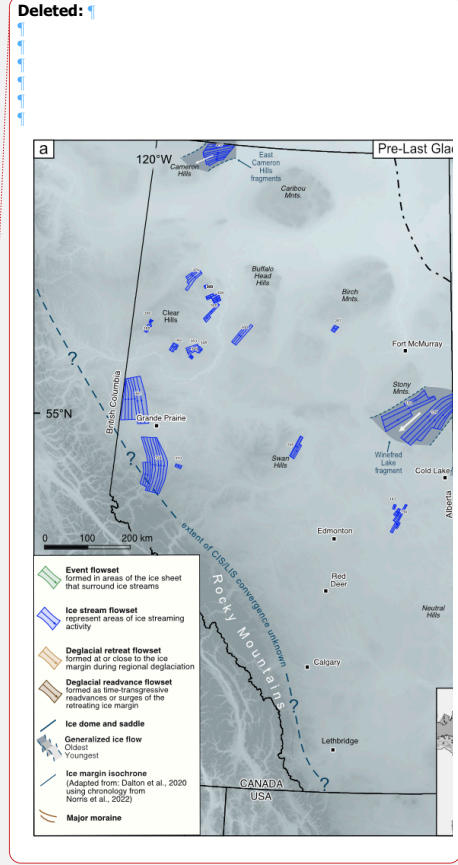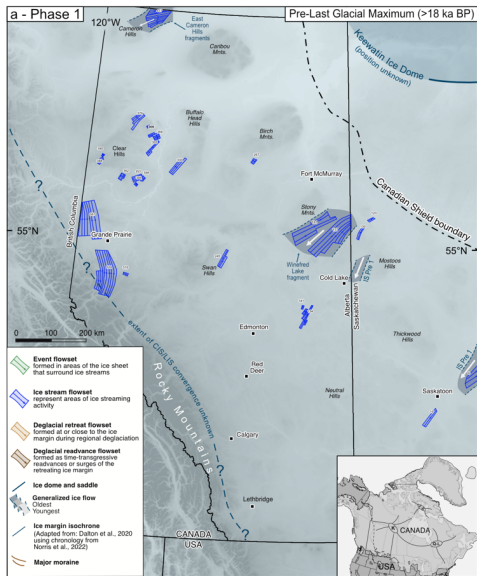
Figure *4*: Deglacial ice flow dynamics of the southwestern Laurentide Ice Sheet. This reconstruction presents a comprehensive synthesis, collating pre-existing ice stream mapping with ice streams presented in this study. Timing of ice retreat and associated ice flow reorganizations are constrained using the deglacial chronology of Norris et al. (2022). Digital elevation model (DEM) from the Shuttle

1510

Note Figure 4 is a five-panel figure; Panel (a) is above and panels (b-e) are below.

... [1]
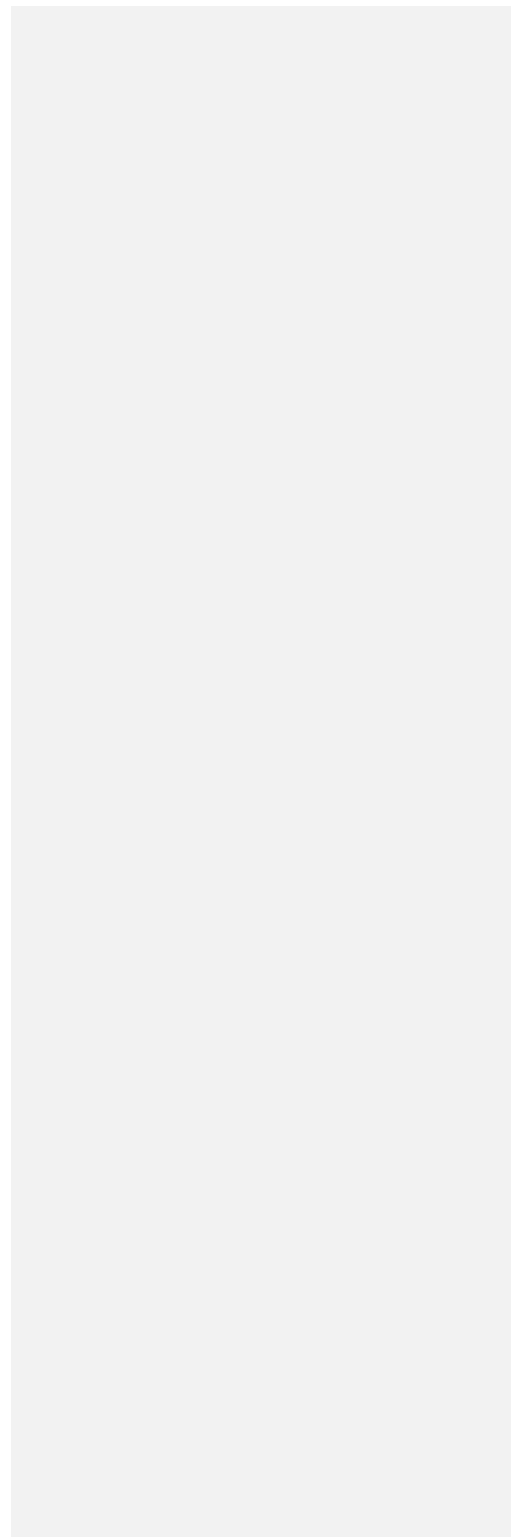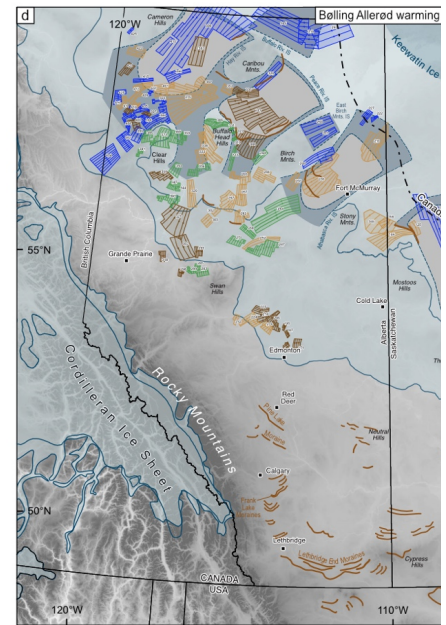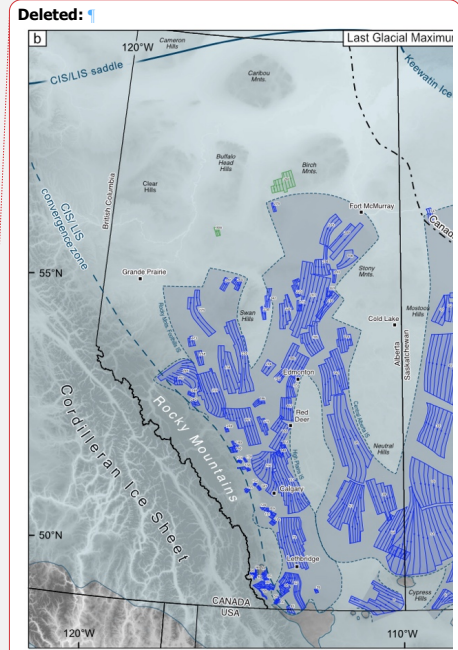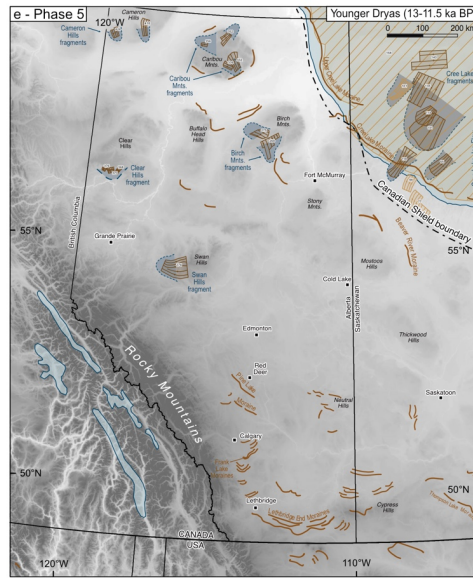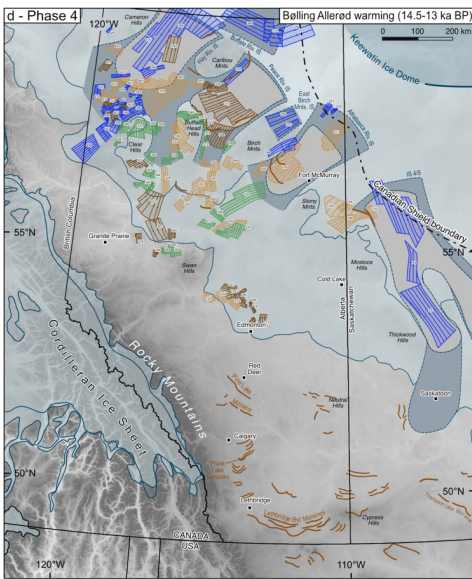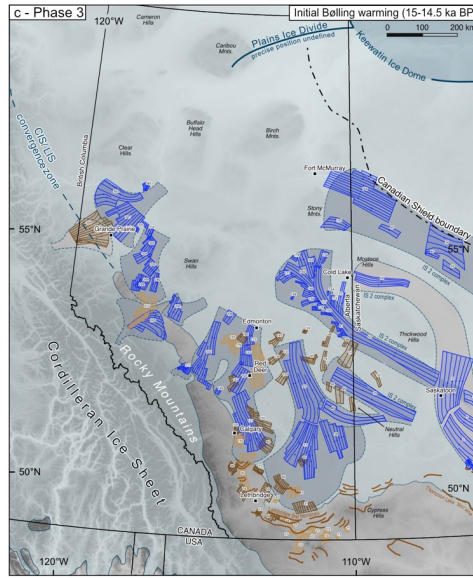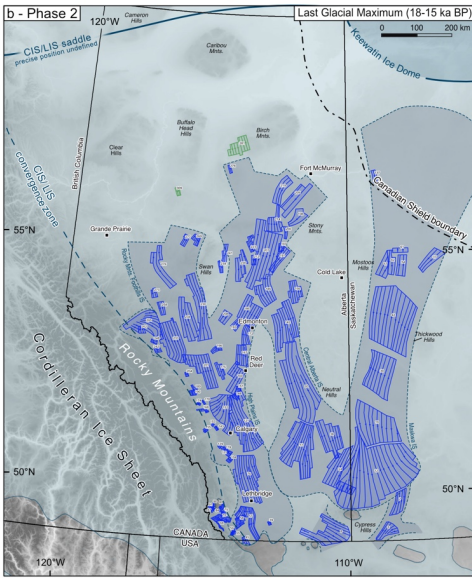
Figure 5: Regional geomorphic imprint of the distribution of ice sheet active retreat and punctuated stagnation across the southwestern

1520 **Laurentide Ice Sheet.** Digital elevation model (DEM) from the Shuttle Radar Topographic Mission (SRTM) provided by the USGS EROS Archive (EROS Centre, 2018). Last glacial maximum ice extent from Dalton et al. (2020).
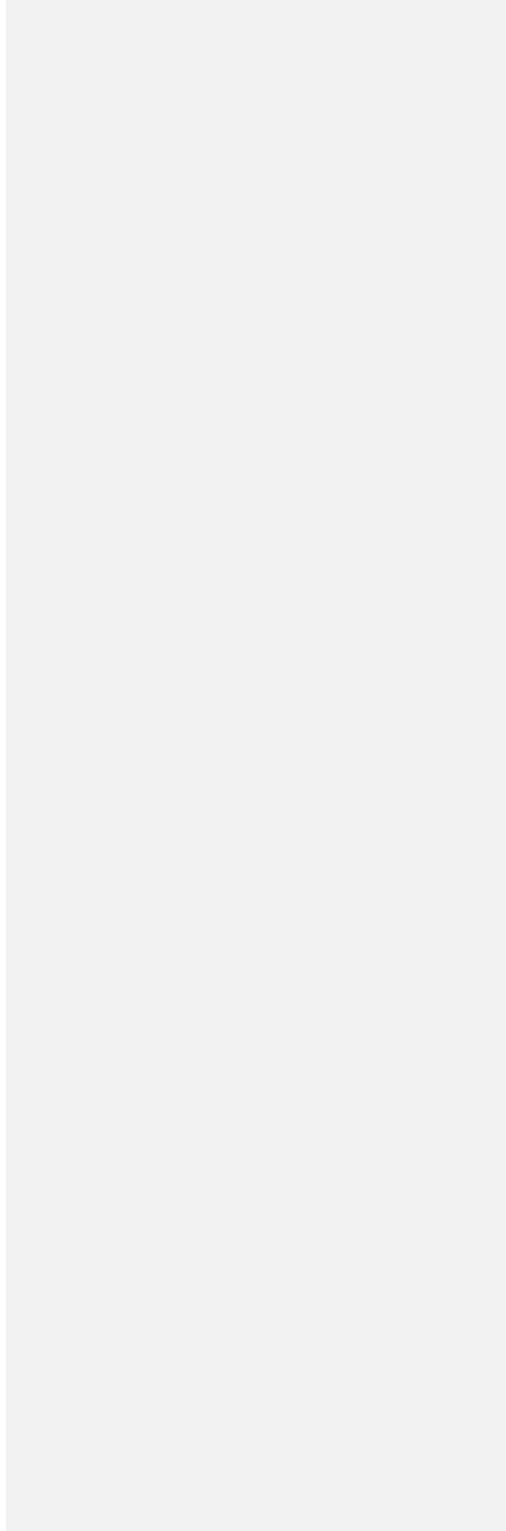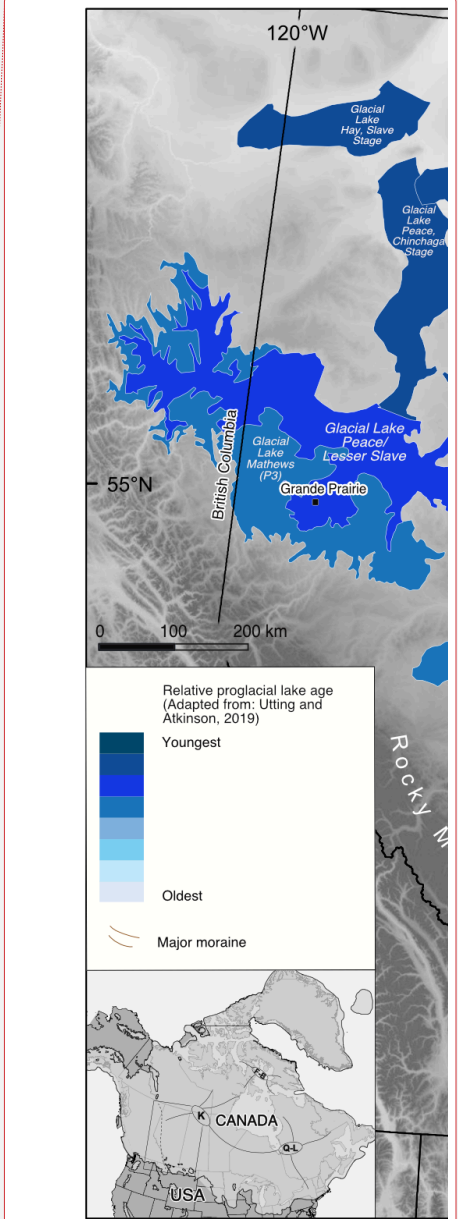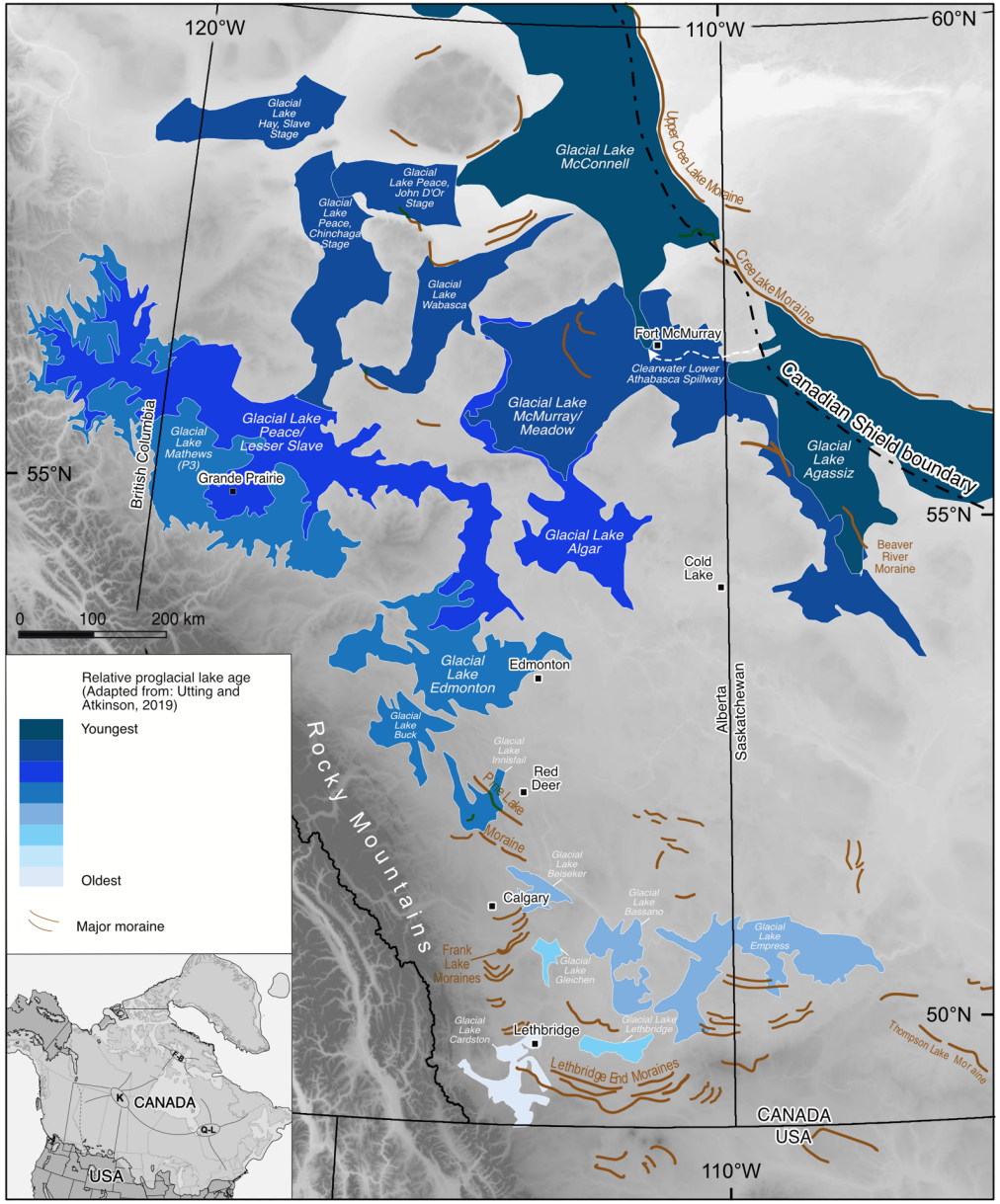
1525   **Figure 6: Distribution of reconstructed proglacial lakes associated with the retreat of the southwestern Laurentide Ice Sheet, classified by relative age, adapted from Utting and Atkinson (2019). Digital elevation model (DEM) from the Shuttle Radar Topographic Mission (SRTM) provided by the USGS EROS Archive (EROS Centre, 2018). Last glacial maximum ice extent from Dalton et al. (2020).**

1530

a INITIAL ICE MARGIN RETREAT
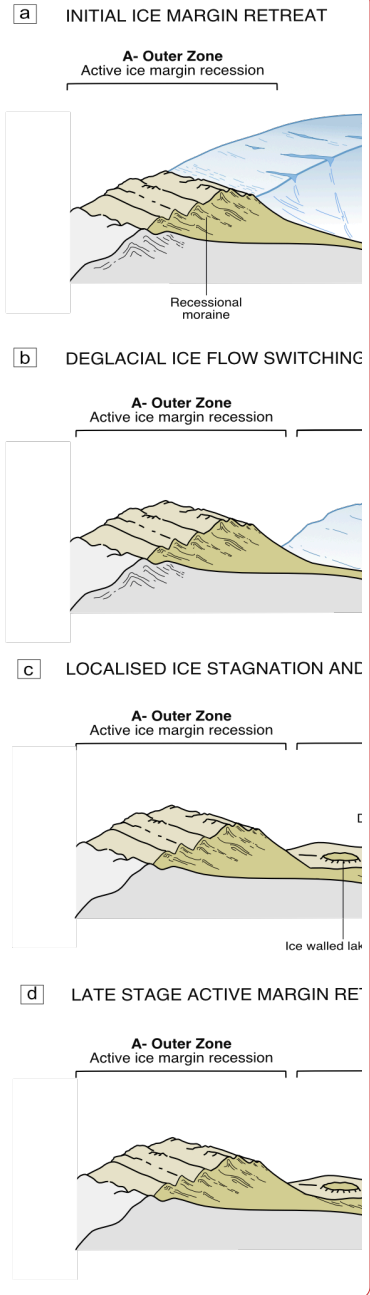
A- Outer Zone
Active ice margin recession

Ice Flow

Recessional
moraine
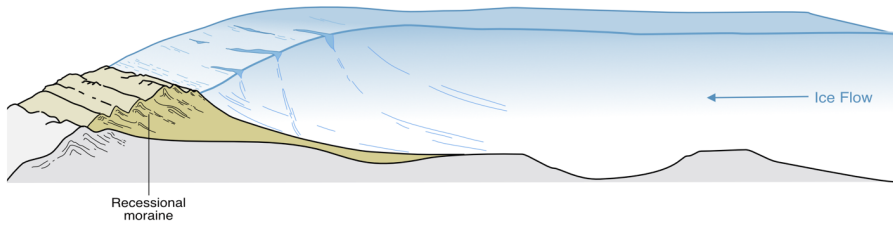
b DEGLACIAL ICE FLOW SWITCHING & ICE MARGIN ISOLATION

A- Outer Zone
Active ice margin recession

B- Intermediate Zone
Ice stagnation and downwasting,

Ice Flow
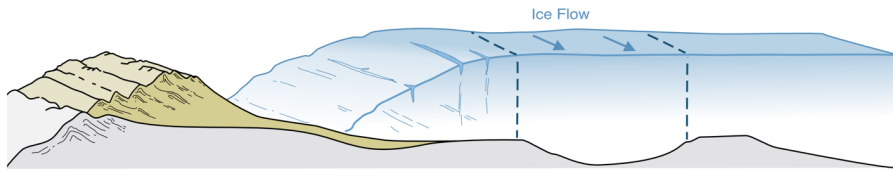
c PUNCTUATED ICE STAGNATION AND DOWNWASTING

A- Outer Zone
Active ice margin recession

B- Intermediate Zone
Ice stagnation and downwasting

Ice Flow

Hummocky
moraine

Localised
glacial surging

Localised
minor
recessional
moraines

Dead-ice

Ice walled lake plain

Proglacial
Lake
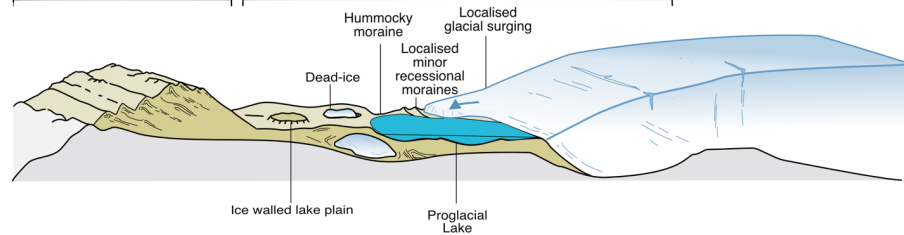
d LATE STAGE ACTIVE MARGIN RETREAT

A- Outer Zone
Active ice margin recession

B- Intermediate Zone
Localised ice stagnation and downwasting

C- Inner Zone
Active ice margin recession

Crevasse-
squeeze
ridge

Esker

Ice Flow

Kettle lake

Glacial
lineation

Recessional
moraine
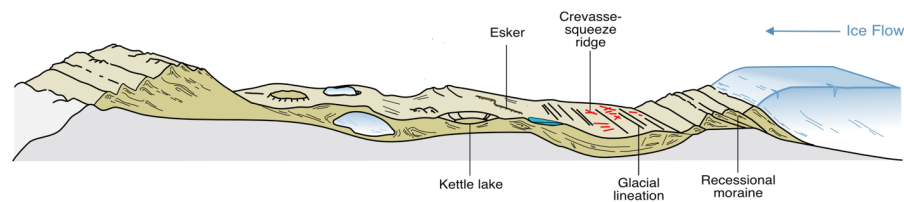
Figure 7: Schematic model of the geomorphic imprint associated with the terrestrial ice sheet margin collapse of the southwestern Laurentide Ice Sheet. (a) Shows initial ice margin retreat in the outer deglacial zone. Large ice streams fed the margin and are orientated perpendicular to the direction of marginal retreat. (b) Shows deglacial ice flow switching and reorganization resulting in the isolation of large regions of the ice sheet in the intermediate deglacial zone. (c) Ice sheet thinning, and rapid retreat triggered macroscale ice stream reorganization, resulting in the isolation of large regions of the ice sheet and ice sheet stagnation in the intermediate deglacial zone. In some locations, stagnation terrain is crosscut by the signature of local small surge events. (d) Shows late-stage active margin retreat of the inner deglacial zone.

Table 1: Diagnostic criteria for identifying flowset types (after Kleman et al., 1997; Stokes and Clark, 1999; Kleman et al., 2006; Greenwood and Clark, 2009).

Flowset types	Characteristics
Ice stream	Represent corridors within an ice sheet that are flowing faster relative to the surrounding ice. Composed of groups of ice flow parallel lineations (drumlinoid ridges, mega-scale glacial lineations (MSGL), and crag-and-tail features) with abrupt lateral margins (in places marked by lateral shear moraines).
Event	Represent areas of ice flow surrounding corridors of fast flow (ice streams). Composed of groups of ice flow parallel lineations (drumlinoid ridges, mega-scale glacial lineations (MSGL), and crag-and-tail features). These flowsets are not associated with meltwater channels, but may contain eskers that overprint the flowset. These eskers are commonly misaligned with the flowset and result from a later stage of deglaciation, which are associated with different flowset orientation.
Deglacial retreat	Represent areas of the ice sheet at or close to the margin that underwent active (warm-based) retreat. Composed of groups of ice flow parallel lineations (drumlinoid ridges, mega-scale glacial lineations (MSGL), and crag-and-tail features) which align locally with eskers and meltwater channels. These flowsets are often associated with terminal, recessional moraines or glaciotectonic thrust ridges.
Deglacial readvance	Represent areas of the ice sheet at or close to the margin that underwent active (warm-based) retreat and were then locally overprinted during a minor readvance or change in ice flow direction during retreat. In some cases, these flowsets may represent switches between periods of rapid and slow ice flow driven by internal forcing mechanisms, in such cases we refer to them as exhibiting surge behaviour. Composed of groups of ice flow parallel lineations (drumlinoid ridges, mega-scale glacial lineations (MSGL), and crag-and-tail features) which align locally with eskers and meltwater channels. These flowsets are often associated with terminal, recessional moraines or glaciotectonic thrust ridges.
Palimpsest	Represent areas that are overprinted by younger ice flows with older flow traces exhibiting a similar orientation. These flowsets are often fragments.
Unknown	Represent areas where the age and significance of landforms are uncertain. These flowsets are often fragments or contain insufficient landforms to interpret their origin.

Page 33: [1] Deleted   Sophie Norris   10/5/23 3:21:00 PM